NIST Technical Note 1972

# Wireless Activities in the 2 GHz Radio Bands in Industrial Plants

Yongkang Liu
Nader Moayeri

This publication is available free of charge from:
https://doi.org/10.6028/NIST.TN.1972

National Institute of
Standards and Technology
U.S. Department of Commerce

**NIST Technical Note 1972**

# Wireless Activities in the 2 GHz Radio Bands in Industrial Plants

Yongkang Liu
Nader Moayeri
*Advanced Network Technologies Division*
*Information Technology Laboratory*

This publication is available free of charge from:
https://doi.org/10.6028/NIST.TN.1972

September 2017

U.S. Department of Commerce
*Wilbur L. Ross, Jr., Secretary*

National Institute of Standards and Technology
*Kent Rochford, Acting NIST Director and Under Secretary of Commerce for Standards and Technology*

**National Institute of Standards and Technology Technical Note 1972**
**Natl. Inst. Stand. Technol. Tech. Note 1972, 42 pages (September 2017)**
**CODEN: NTNOEF**

**This publication is available free of charge from:**
**https://doi.org/10.6028/NIST.TN.1972**

**Abstract**

Wireless connections are becoming popular in industrial environments that increasingly carry sensing and actuation data over the air. In industrial plants, activities of legacy wireless systems have shaped the channel usage in the radio spectrum bands for new wireless applications. The 2 GHz spectrum band consists of a good number of radio resources that are dedicated to fixed and mobile wireless communications. In this report, passive measurement data collected in two industrial plants is analyzed to identify existing wireless activities in this frequency band. Besides, a statistical channel usage model is developed for the 2.4 GHz Industrial, Scientific and Medical (ISM) band. The secondary spectrum utility is evaluated given legacy wireless activity in the ISM band, which is of particular interest to unlicensed industrial wireless networking standards, such as WirelessHART and ISA100.11a.

**Key words**

Communication channels, radio spectrum measurement, industrial plants.

## Table of Contents



## List of Tables

**List of Figures**

# 1. Introduction

## 1.1. 2 GHz Frequency Band

The 2 GHz frequency band is of great interest to wireless applications due to its good radio propagation characteristics and the availability of licensed and unlicensed resources for wireless communications. It includes the popular unlicensed 2.4 GHz ISM band. However, new players have to share the bandwidth with existing radio users ranging from wireless local area networks (WLAN), low power wireless sensor networks and satellite communications. Therefore, a thorough survey of on-site spectrum usage is warranted to explore the intensity of the legacy wireless activities and to prepare for coexistence with new radios to be deployed. In this report, we capture the features of wireless activities in time, frequency and space through analysis of passive channel measurements made at two industrial facilities. After identifying the signals that may cause interference to new users of this band, we characterize the time variation of channel occupancy by a Markov chain and obtain its statistical parameters.

## 1.2. Passive Spectrum Measurement Settings

On-site passive measurements were made in two manufacturing facilities, i.e., the National Institute of Standards and Technology (NIST) machine shop located in Gaithersburg, Maryland and an automotive transmission assembly plant in Detroit area, Michigan. While the former has many common features of small-to-medium size manufacturing sites, the latter is a typical plant layout for large-scale manufacturing. Two rounds of passive measurements were made in each plant, one for each listening spot used. Each measurement lasted a few hours, as specified in Table 1. The data is also available online as the part of a NIST “Wireless Systems for Industrial Environments” website [1].

**Table 1.** Specifications of Passive Measurements Made in Two Industrial Plants.

| Listening Spot | Site | | | |
|---|---|---|---|---|
| | NIST Machine Shop | | Automotive Assembly Plant | |
| | P1a | P1b | P2a | P2b |
| Start Time | 07:32:16 AM 04/07/2015 | 02:00:11 PM 04/07/2015 | 04:53:51 PM 04/14/2015 | 04:03:59 PM 04/13/2015 |
| End Time | 01:32:45 PM 04/07/2015 | 11:09:39 AM 04/08/2015 | 05:12:08 PM 04/15/2015 | 04:04/53 PM 04/14/2015 |
| Spot Notes | Middle South of the plant | West North of the plant | TX2 position (P10_Q10) | TX1 position (M18) |

Each passive measurement was made in the frequency range 2.1 GHz to 2.8 GHz by a spectrum analyzer that remained in one spot for a few hours. Each sweep over the observed spectrum takes about 2.3 s, including both frequency scanning period (about 0.1 s) and data processing. The measured band is broken into 7000 frequency bins, each of which 100 kHz wide. In each sweep, the received signal strength indicator (RSSI) in each single bin is saved in dBm.

The data set of the RSSI readings at one spot is stored in a 2-D matrix

$$A = \begin{bmatrix} \alpha_{1,1} & \alpha_{1,2} & \cdots & \alpha_{1,N_B} \\ \alpha_{2,1} & \alpha_{2,2} & & \alpha_{2,N_B} \\ \vdots & & \ddots & \vdots \\ \alpha_{N_T,1} & \alpha_{N_T,2} & \cdots & \alpha_{N_T,N_B} \end{bmatrix} \tag{1}$$

which contains $N_T$ continuous sweeps (rows) over $N_B$ frequency bins (columns). Each element, $\alpha_{i,j}$, represents the RSSI reading in dBm in the j-th frequency bin at the i-th sweep.

Any wireless channel occupying more than 100 kHz of spectrum band is made up of a number of contiguous frequency bins. For example, the IEEE 802.11b channel has a bandwidth of 22 MHz that spans over 220 bins (columns) in the data set. Therefore, the RSSI of a given channel is computed by adding the RSSIs of all the bins comprising the channel. If the channel spans over the bins in columns $\{f_s, f_{s+1}, \ldots, f_{t-1}, f_t\}$, then the total channel RSSI in dBm at sweep $i$ is given by

$$S_i = 10log_{10}(\sum_{j=f_s}^{f_t} 10^{\frac{\alpha_{i,j}}{10}}) \tag{2}$$

In what follows, an analysis is performed on each data set $A$ to identify all wireless activities in the frequency band of interest and to characterize the burstiness of each channel identified. In addition, the difference between wireless activities observed at different spots will be discussed.

### 1.3. Organization

This report is made up of two parts. In the first part, we briefly introduce the passive measurements made at two industrial plants and present initial observations on spectrum usage in the frequency range 2.1 GHz to 2.8 GHz at the two listening spots used. In the second part, we focus on the 2.4 GHz ISM band. From the perspective of a potential WLAN user, transmission opportunities in various WLAN channels are identified. We model the channel occupancy by a Markov chain and compute its statistical transition parameters.

## 2. Wireless Activities in the 2 GHz Radio Bands

FCC has allocated a number of licensed and unlicensed UHF bands in the frequency range 2.1 GHz to 2.8 GHz for fixed and mobile wireless communications [1]. The key to detect active wireless usage in each sweep is to identify the bins with active signal transmissions as opposed to those with noise power present only. These are called ON and OFF bins, respectively. Note that the power level in each frequency bin varies over time. Therefore, it is difficult, if not impossible, to identify all the bins that belong to an active channel at any given time, especially when the channel noise distribution is unknown a priori. Our analysis begins with processing measurement data to illustrate the correlation between bins adjacent in the frequency domain.

For a given bin RSSI threshold μ and any $\alpha_{i,j}$ in $A$, the indicator function $d_{i,j}$ is defined as

$$d_{i,j} = \begin{cases} 0, & if\ \alpha_{i,j} < \mu \\ 1, & otherwise \end{cases}.$$

Bin $i$ is marked as ON checked active at sweep $j$, if $d_{i,j} = 1$, and OFF otherwise. Note that the ON/OFF designation highly depends on the choice of μ. Since each bin has $N_T$ RSSI readings in $A$, $0 \leq \sum_{i=1}^{N_T} d_{i,j} \leq N_T$.

It is plausible to assume the more frequently a bin is marked as active, the more likely it is that some wireless user is using it in the vicinity of the measurement location. Thus, an active channel can be identified as a group of contiguous bins that exhibit a higher chance of being active than the neighboring bins. In other words, given μ, if a bin has a larger $\sum_{i=1}^{N_T} d_{i,j}$, then the bin is more likely to carry active signals during the measurements. Consequently, an active spectrum band at the listening spot tends to include a set of contiguous bins with larger $\sum_{i=1}^{N_T} d_{i,j}$ values than those in the unused bins.

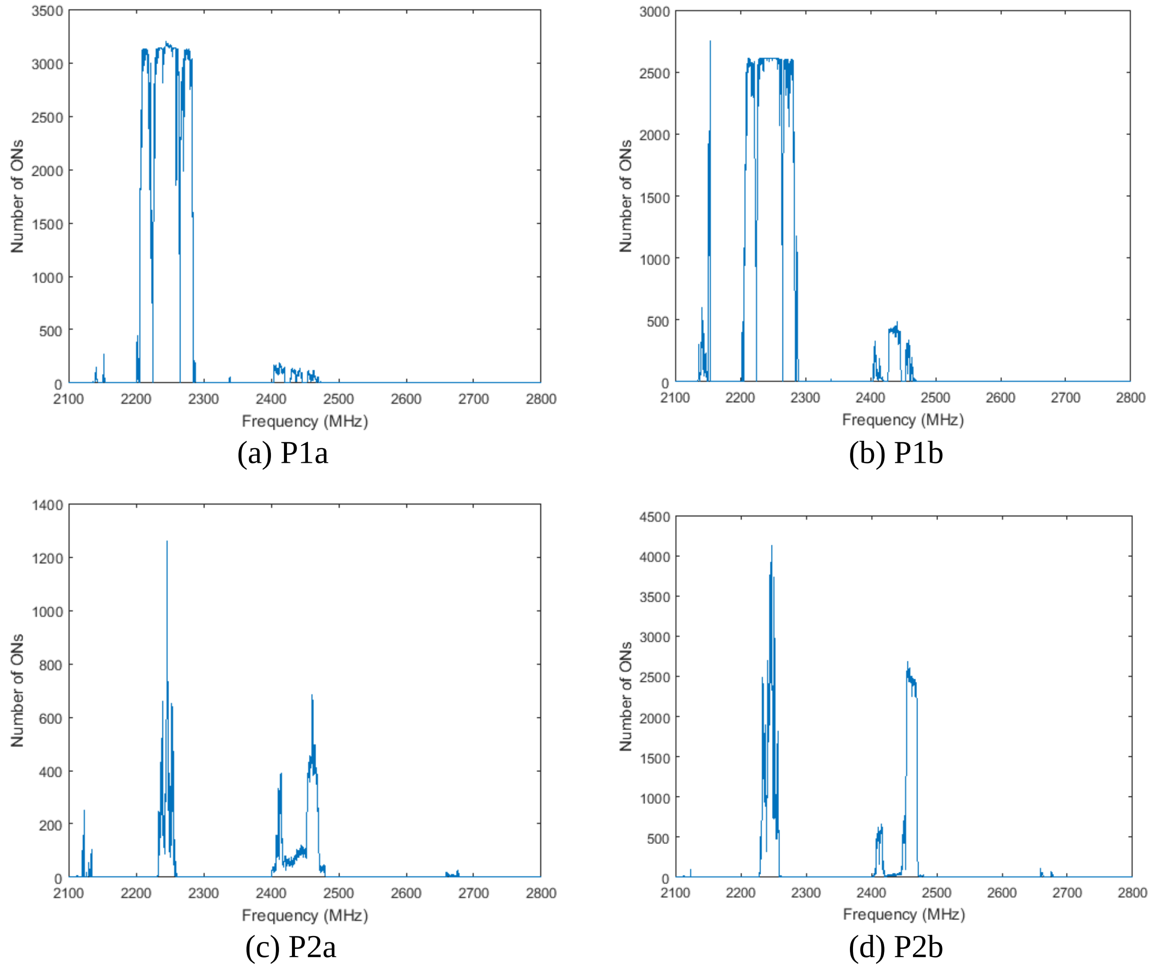


**Fig. 1.** Total number of times a bin was ON as a function of frequency at various listening spots ($\mu = -80\ dBm$)

Figure 1 plots $\sum_{i=1}^{N_T} d_{i,j}$ as a function of frequency for μ = -80 dBm. The distribution of active bins can be used as an indication of wireless usage in the identified frequency bands because 1) the threshold μ filters out most unused bins with RSSI values corresponding to noise and passes the signal bins with higher RSSI intensity, and 2) counting over time (all sweeps) highlights the frequency bands that are more frequently used.

We checked the radio spectrum regulations, such as FCC's in the USA, for the bands used in the 2.1 GHz to 2.8 GHz range. The spectrum bands identified as active at the measurement sites are listed in Table 2.

Table 2 indicates that the use of various bands at the two industrial sites is similar, except for the 2320 MHz to 2345 MHz band which is only used in the first site and the 2655 MHz to 2690 MHz band which is only used in the second one. It is also true that the two listening spots at each site exhibit the same usage behavior. However, in the same plant, it is worthwhile to note that the strength of the received wireless signals varies due to factors such as RF propagation properties at a given site and the distances to signal sources. Admittedly, there might be more active bands that are not listed in Table 2, because the signal received in these "silent" bands were either too weak compared with the background noise or happened to be absent during the measurement period. In the following subsections, the features of wireless usage for each spectrum band in Table 2 is discussed.

**Table 2**. Specifications of active wireless bands in passive measurements

| Band | Frequency Range (MHz) | FCC Usage Regulations on Frequency Allocations | Visibility | | | |
|---|---|---|---|---|---|---|
| | | | P1a | P1b | P2a | P2b |
| 1 | 2110-2155 | • Fixed point-to-point microwave and mobile communications (FCC AWS-1 block A-F) | O | O | O | O |
| 2 | 2200-2290 | • Space operations (space-to-Earth) (space-to-space)<br>• Earth exploration - Satellite (space-to-Earth) (space-to-space) (line-of-sight only)<br>• Mobile (line-of-sight only including aeronautical telemetry, but excluding fixed wireless communications flight testing of manned aircraft)<br>• Space research (space-to-Earth) (space-to-space) | O | O | O | O |
| 3 | 2320-2345 | • Satellite broadcasting | O | O | × | × |
| 4 | 2400-2500 | • Wireless communications for ISM Equipment | O | O | O | O |
| 5 | 2655-2690 | • Radio astronomy<br>• Fixed wireless communications<br>• Mobile except aeronautical mobile | × | × | O | O |

### 2.1. Band 1: 2110 MHz to 2155 MHz

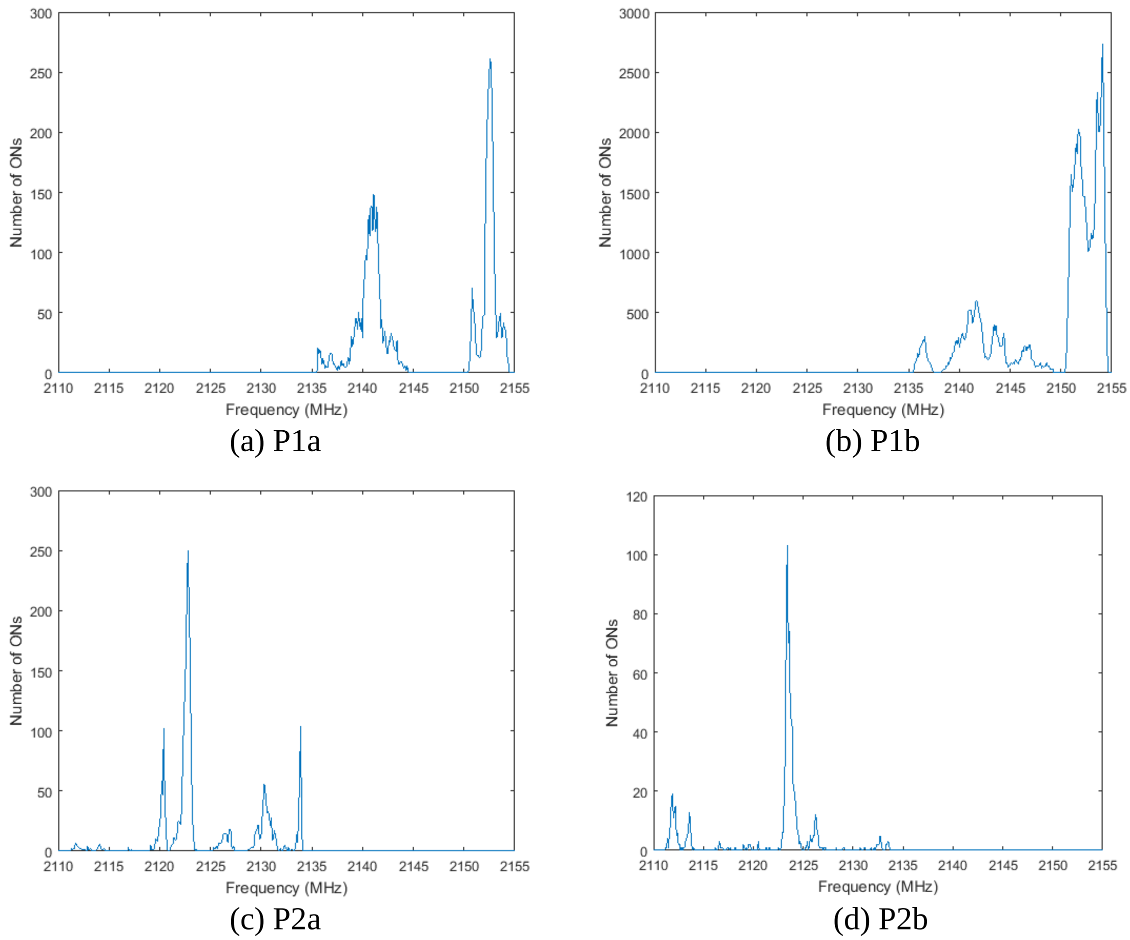


**Fig. 2.** Number of ON bins in Band 1 at individual listening spots ($\mu = -80\ dBm$)

FCC allocates the frequencies from 2110 MHz to 2155 MHz for fixed and mobile wireless communications. Activities in this frequency range have been observed at all four locations as shown in Fig. [2]. The range of frequencies observed at the two plants is slightly different, but listening spots in the same plant report the same frequency ranges, which suggests that both spots in a given plant captured activities from the same signal source. However, such frequency domain responses do not address time evolution of wireless activities. To better understand channel usage variation as a function of time, time domain analysis is performed next.

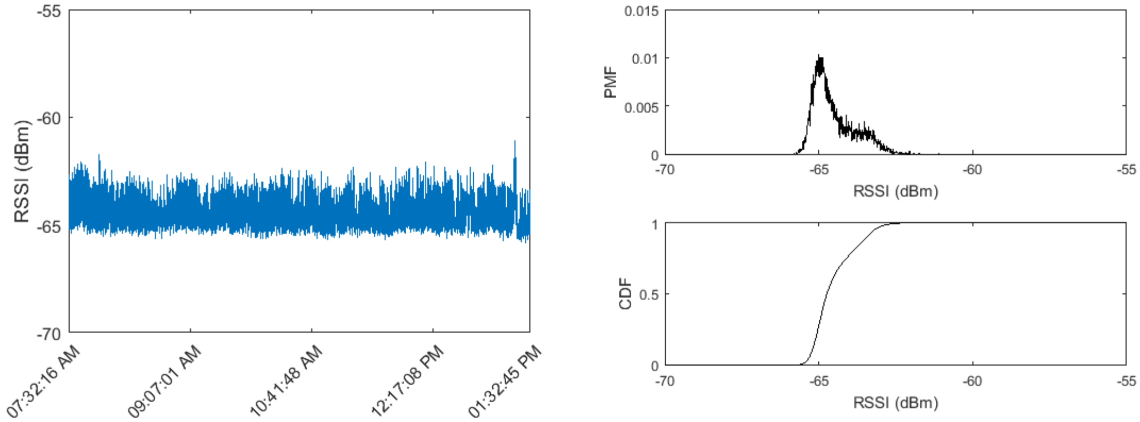


(a) P1a

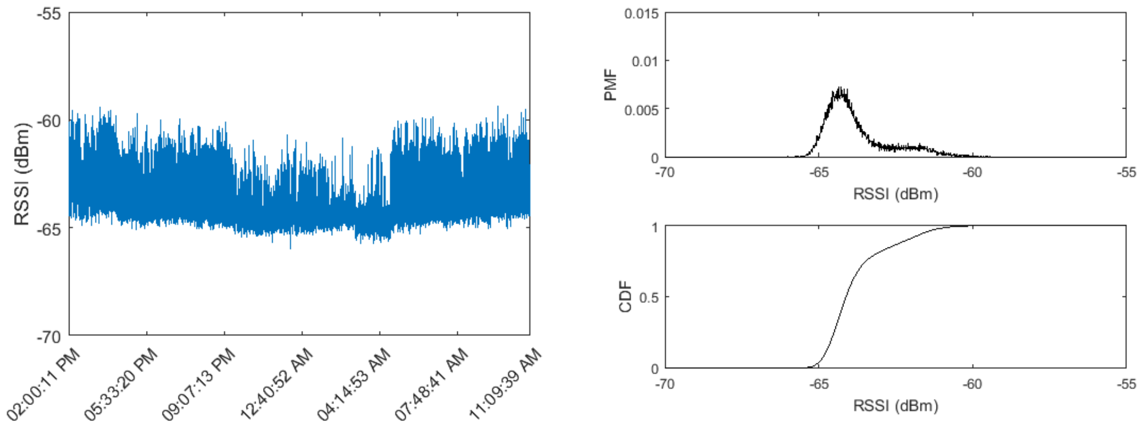


(b) P1b

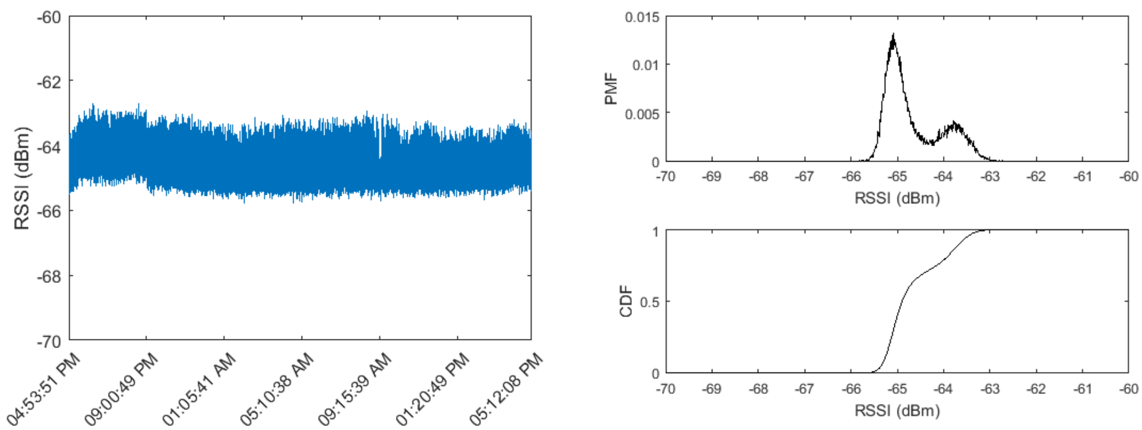


(c) P2a

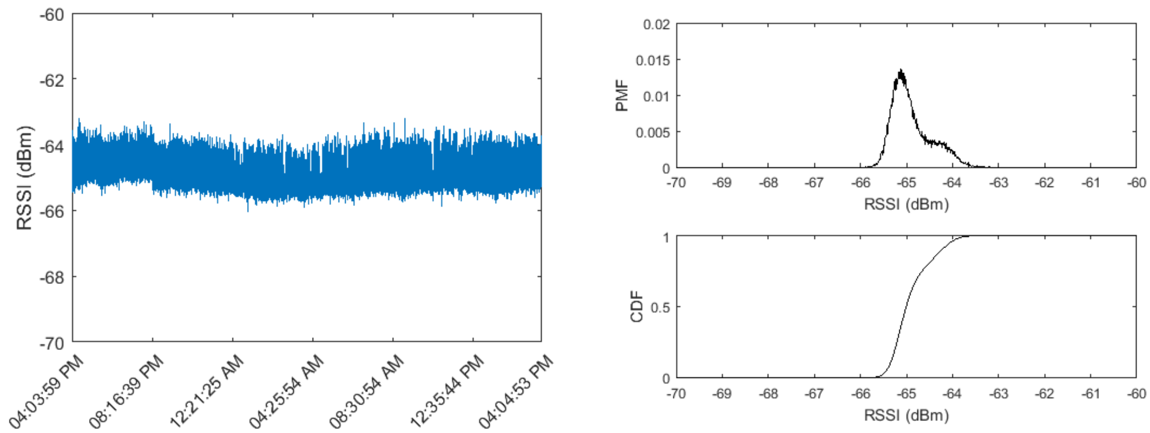


(d) P2b

**Fig. 3.** Time variations (LEFT Col.) and statistics (RIGHT Col.) of RSSI in Band 1 at different listening spots

Figure 3 illustrates the temporal variations of RSSI in Band 1 and the statistical distribution of RSSI at each location. The RSSI in Band 1 in each sweep is calculated using Eq. (2) in the frequency range of 2110 MHz to 2155 MHz. It indicates that the channel usage is dispersive during the measurements. The curves of probability mass function (PMF) and cumulative distribution function (CDF) also confirm the existence of signal transmissions with higher RSSI values beyond the noise.

According to FCC spectrum rules, the 2110 MHz to 2155 MHz band is the downlink band of advanced wireless services (AWS) block A-F (AWS-1), which is paired with the 1710 MHz to 1755 MHz uplink band[1]. Cellular carriers are licensed to operate commercial cellular services, e.g., 3GPP long-term evolution (LTE), in this band.[2] The NIST machine shop is located on the NIST Gaithersburg campus, Montgomery County, Maryland. In the local license map from the FCC online spectrum dashboard, Block A (2110-2120 MHz) is licensed to AT&T; Blocks B (2120-2130 MHz) and C (2130-2135 MHz) are licensed to Verizon; and Blocks D (2135-2140 MHz), E (2140-2145 MHz) and F (2145-2155 MHz) are licensed to T-Mobile.[3] Carriers can allocate channels with bandwidth of 1.4, 3, 5, 10, 15, or 20 MHz in the licensed band. During the measurements at P1a and P1b, the active usage of Blocks D, E and F (licensed to T-Mobile) has been captured. As the carrier occupies three adjacent block bands, the operator may aggregate them for larger bandwidth. Peaks of signal activities are found at around 2140 MHz and 2150 MHz in the NIST machine shop and at around 2120 MHz and 2130 MHz in the automotive plant.

It is worthwhile to examine the time variations and usage statistics of various frequency blocks in the 2110 MHz to 2155 MHz frequency band separately. Take the NIST locations as an example. Figure 2(a) illustrates that two distinct frequency bands are in use at Loc. P1a. The

[1] Certain commercial entities, equipment, or materials may be identified in this document in order to describe an experimental procedure or concept adequately. Such identification is not intended to imply recommendation or endorsement by the National Institute of Standards and Technology, nor is it intended to imply that the entities, materials, or equipment are necessarily the best available for the purpose.
[2] https://en.wikipedia.org/wiki/LTE_frequency_bands; https://www.fcc.gov/general/advanced-wireless-services-aws; http://www.naic.edu/~phil/rfi/awsbandplan.pdf
[3] http://reboot.fcc.gov/spectrumdashboard/searchMap.seam

left one occupies Blocks D and E and the right one the upper 5 MHz of Block F. Figure 2(b) suggests another possibility of channel allocation, i.e., the left frequency band occupies Blocks D, E and the lower 5 MHz of Block F and the right one the upper 5 MHz of Block F. Figure 4 and Figure 5 illustrate the time variations and statistics of the RSSI in the possible channels at P1a and P1b, respectively.

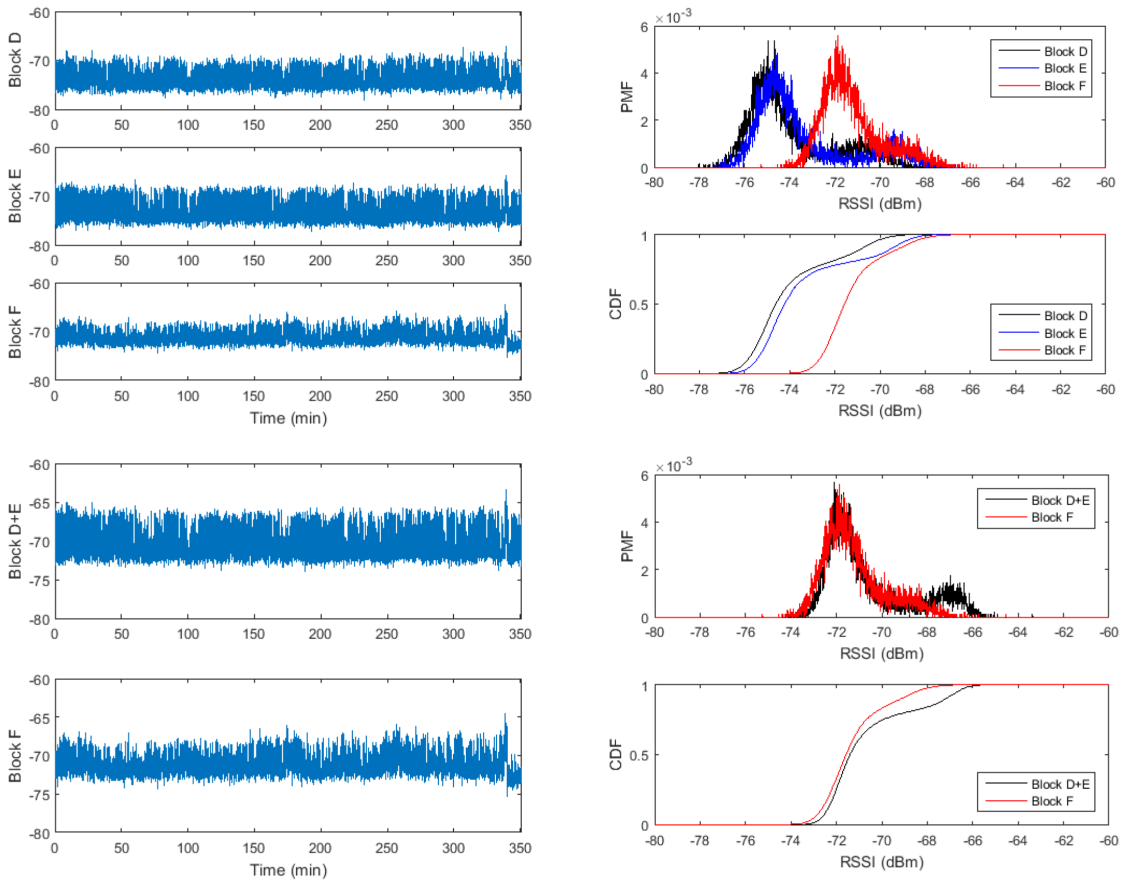


**Fig. 4.** Time variations (LEFT) and statistics (RIGHT) of RSSI (dBm) in the AWS-1 Block D, E, F and aggregated D+E bands at Loc. P1a

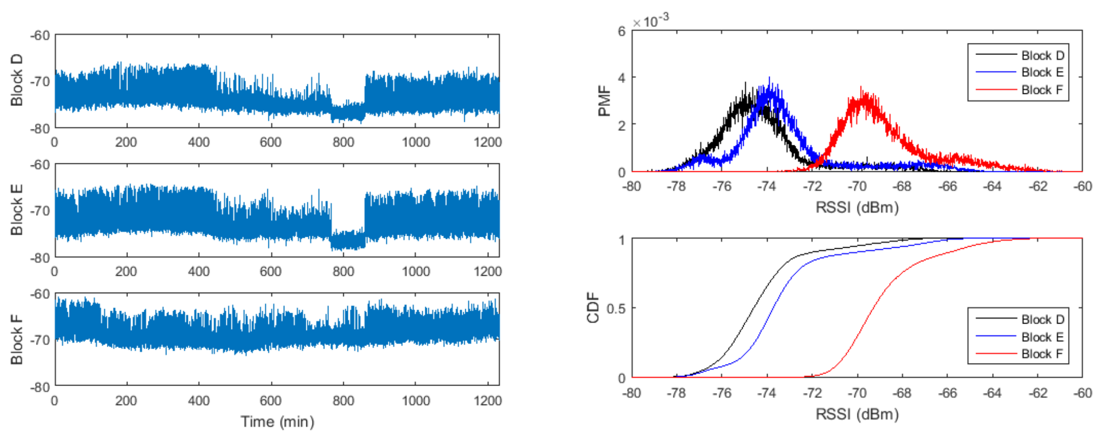

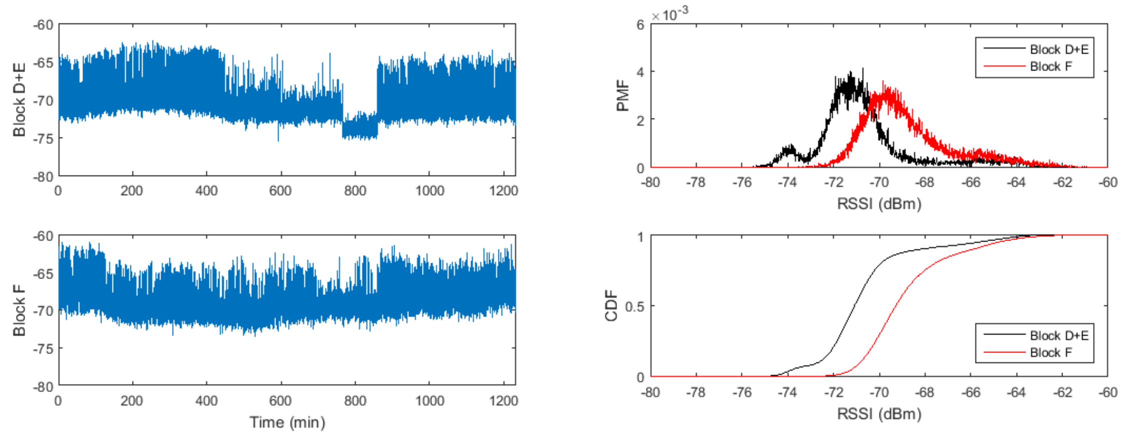


**Fig. 5.** Time variations (LEFT) and statistics (RIGHT) of RSSI (dBm) in the AWS-1 Block D, E, F and aggregated D+E bands at Loc. P1b

Figure 4 suggests that Blocks D and E are aggregated and used together at Loc. P1a, because the time variations of RSSI for these two blocks look similar and so does the PMFs. The time variations of RSSI at Loc. P1b (see Fig. [5]) for Blocks D and E exhibit a time period of clear inactivity around 800 minutes and the time variations for the two blocks are similar at other times. The PMFs, however, are not as similar as in Fig. [4]. Since no a priori information is available on how T-Mobile defines its channels, no conclusion on the multi-channel usage can be made based on the available data. Further measurements and site surveys could help resolve the channelization problem in the future.

## 2.2. Band 2: 2200 MHz to 2290 MHz

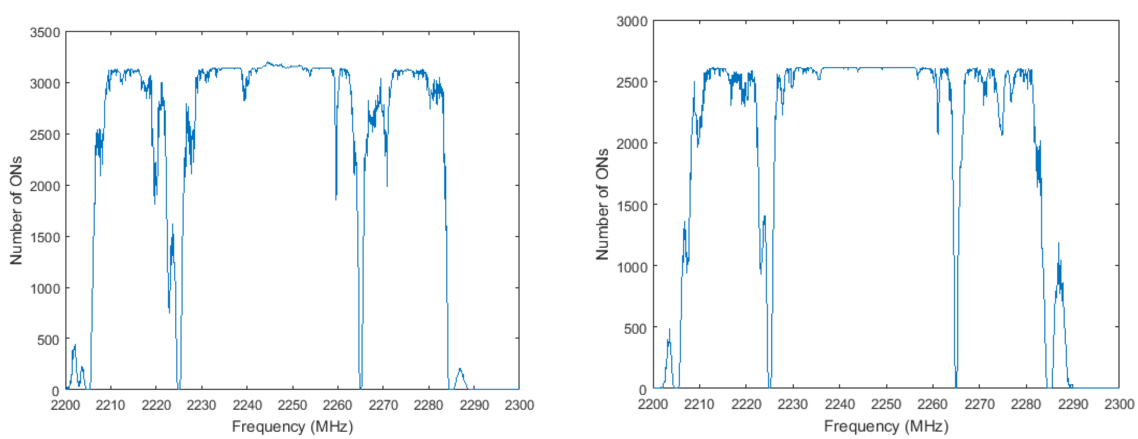


(a) P1a (b) P1b

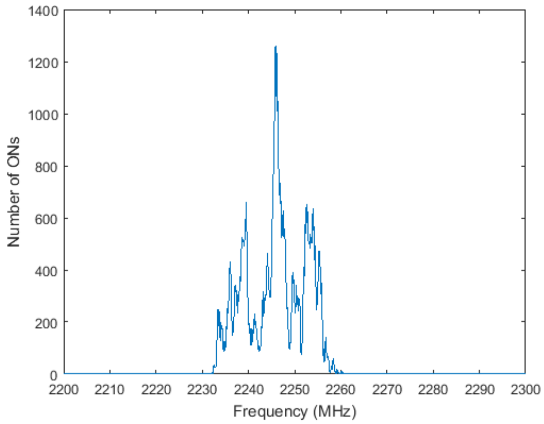


(c) P2a

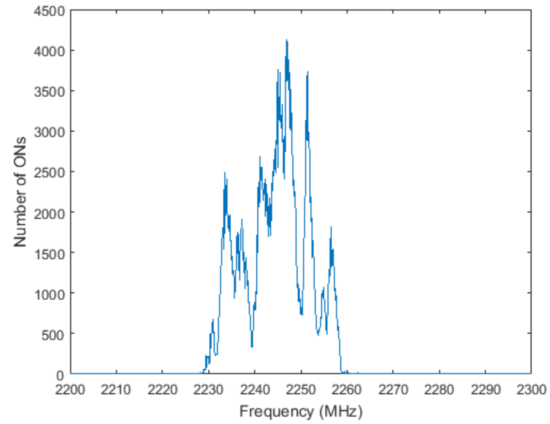


(d) P2b

**Fig. 6.** Number of ON bins in Band 2 at individual listening spots ($\mu = -80\ dBm$)

In the FFC table [2], the band in the frequency range 2200 MHz to 2290 MHz is used for multiple purposes including space research/operation (space-to-earth and space-to-space), satellite communications in earth exploration (space-to-earth and space-to-space), terrestrial fixed (line-of-sight only), and mobile communications (line-of-sight only including aeronautical telemetry, but excluding flight testing of manned aircraft). At both sites, active spectrum usage was observed during the measurements as shown in Fig. [6]. The data is processed in a manner similar to that used to analyze Band 1 and the results are shown in Fig. [7-10] for individual measurements. Some key observations are noted here. First, the band usage in time is bursty. Active periods are usually detected in clusters with short silent gaps in between and last for a few minutes or longer. After the active periods, usually a much longer silent period follows. Second, this band is apparently used as a single broadband channel. Spectrum usage is symmetric in frequency including the main lobe centered at 2245 MHz and sidelobes distributed evenly on both sides. Time evolutions of RSSI in individual lobes validate that active bins at each sweep are associated with the usage in the same single channel.

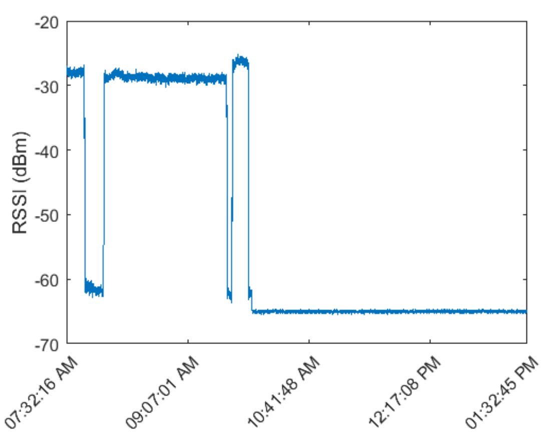


(a) Time variation of RSSI in Band 2

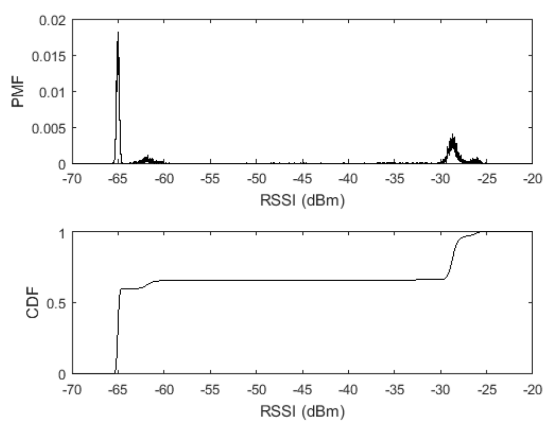


(b) Statistics of RSSI in Band 2

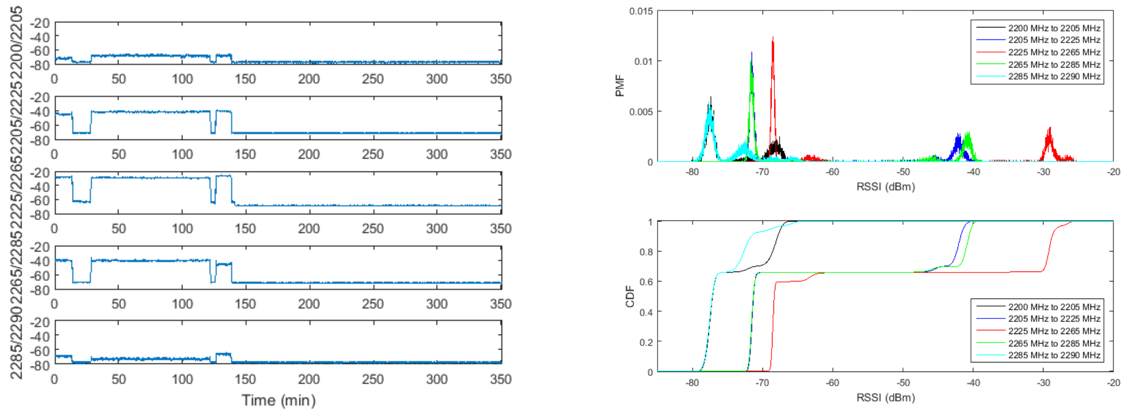


(c) Time variations of RSSI in sub-bands (d) Statistics of RSSI in sub-bands

**Fig. 7.** Time variations and statistics of RSSI (dBm) in Band 2 at Loc. P1a (main lobe: 2225 MHz to 2265 MHz, 1st sidelobes: 2205 MHz to 2225 MHz and 2265 MHz to 2285 MHz, 2nd sidelobes: 2200 MHz to 2205 MHz and 2285 MHz to 2290 MHz)

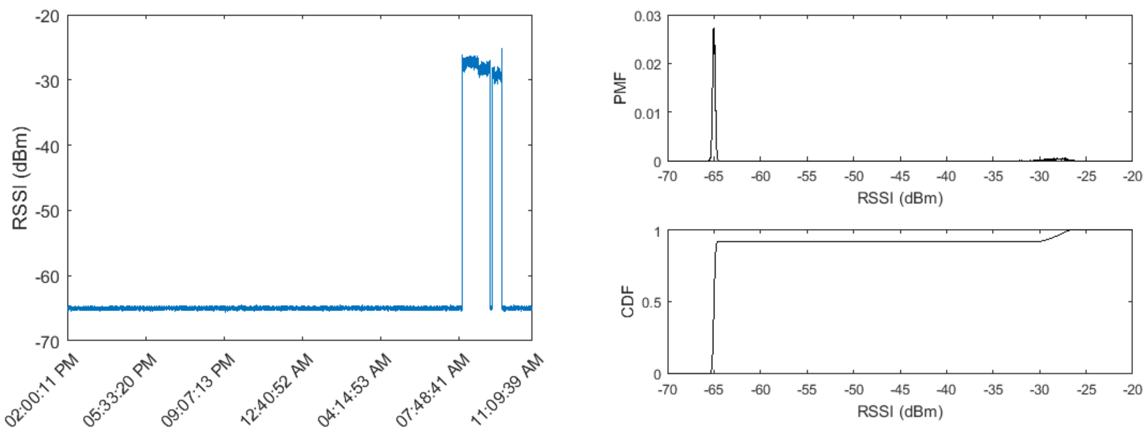


(a) Time variation of RSSI in Band 2 (b) Statistics of RSSI in Band 2

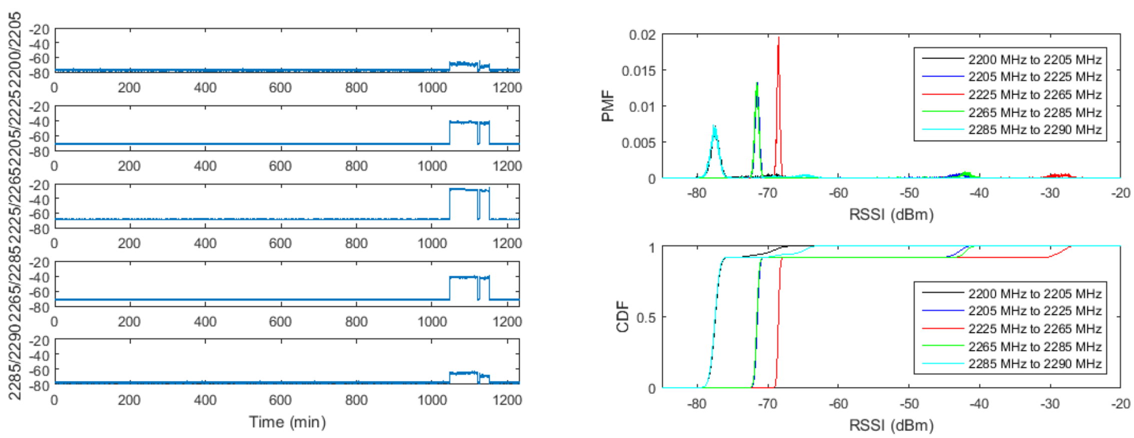


(c) Time variations of RSSI in sub-bands (d) Statistics of RSSI in sub-bands

**Fig. 8.** Time variations and statistics of RSSI (dBm) in Band 2 at Loc. P1b (main lobe: 2225 MHz to 2265 MHz, 1st sidelobes: 2205 MHz to 2225 MHz and 2265 MHz to 2285 MHz, 2nd sidelobes: 2200 MHz to 2205 MHz and 2285 MHz to 2290 MHz)

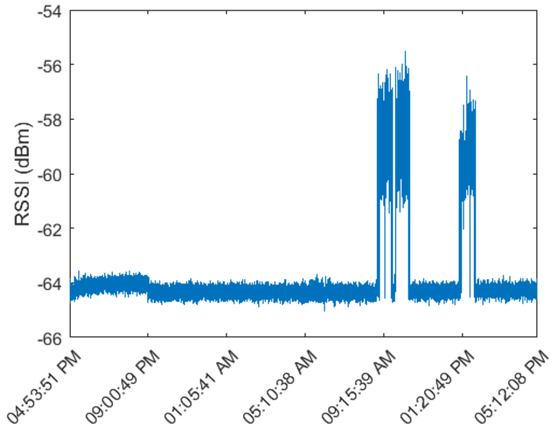


(a) Time variation of RSSI in Band 2

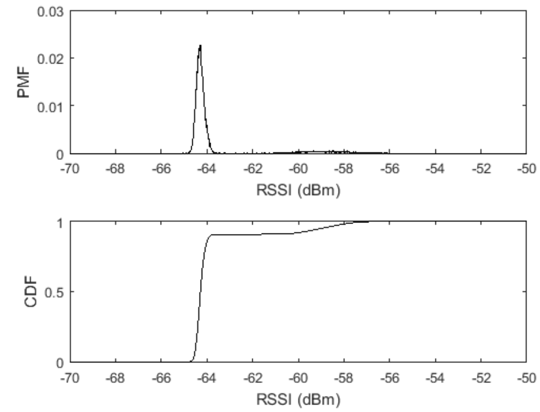


(b) Statistics of RSSI in Band 2

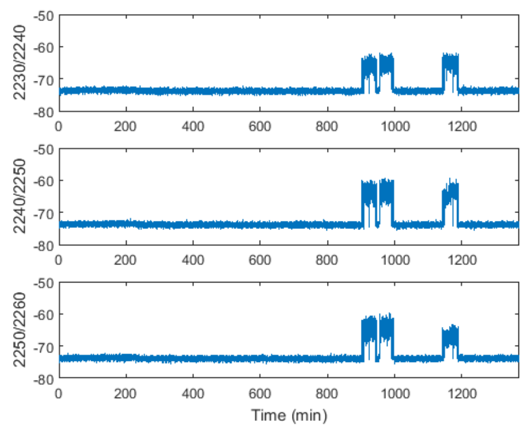


(c) Time variations of RSSI in sub-bands

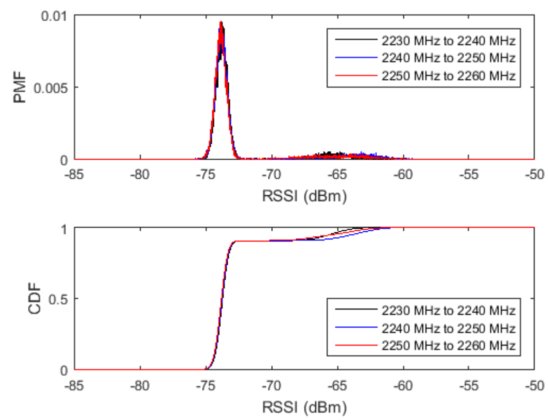


(d) Statistics of RSSI in sub-bands

**Fig. 9.** Time variations and statistics of RSSI (dBm) in Band 2 at Loc. P2a (main lobe: 2240 MHz to 2250 MHz, sidelobes: 2230 MHz to 2240 MHz and 2250 MHz to 2260 MHz)

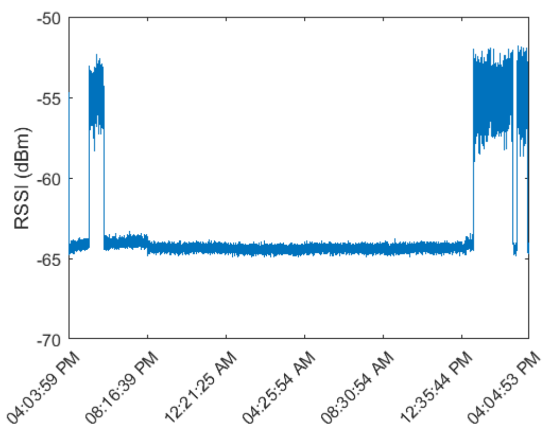


(a) Time variation of RSSI in Band 2

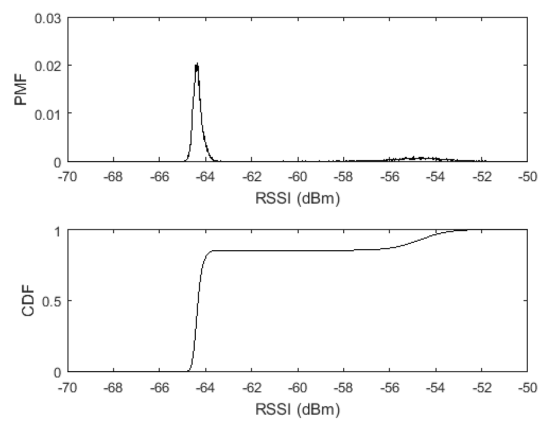


(b) Statistics of RSSI in Band 2

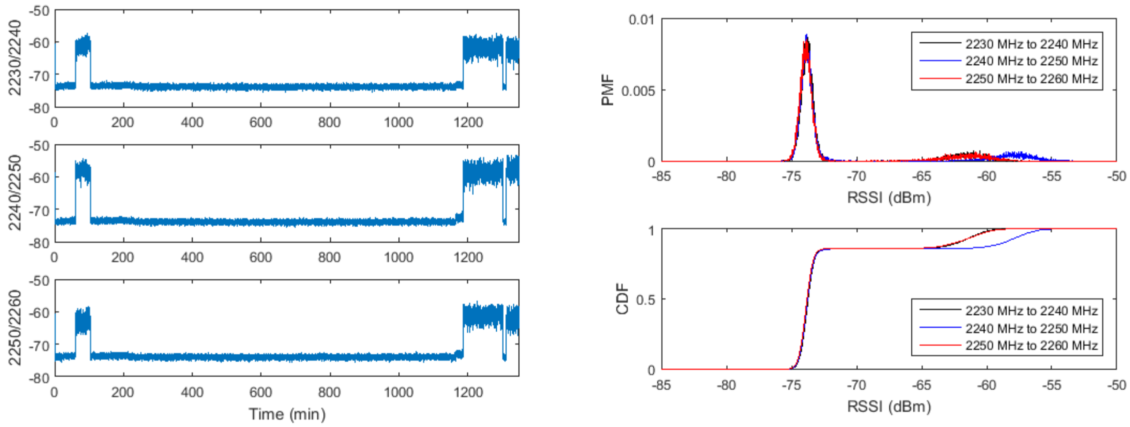


(c) Time variations of RSSI in sub-bands (d) Statistics of RSSI in sub-bands

**Fig. 10.** Time variations and statistics of RSSI (dBm) in Band 2 at Loc. P2b (main lobe: 2240 MHz to 2250 MHz, sidelobes: 2230 MHz to 2240 MHz and 2250 MHz to 2260 MHz)

### 2.3. Band 3: 2320 MHz to 2345 MHz

The measurements at the NIST machine shop also captured some weak signal footage in the 2320 MHz to 2345 MHz band as shown in Fig. [11]. According to the table of frequency allocations, FCC has assigned this band to Sirius XM radio channels for satellite radio programs. Sirius satellites broadcast within the frequencies from 2320.00 MHz to 2332.50 MHz, while XM radio uses adjacent frequencies 2332.50 MHz to 2345.00 MHz [3]. As the satellite reception is very weak within buildings, it is very difficult to distinguish signal activity from noise. The RSSI distribution in Fig. [12] confirms this. Therefore, the energy detection-based measurement data used in this report does not provide any further information about spectrum usage in this band.

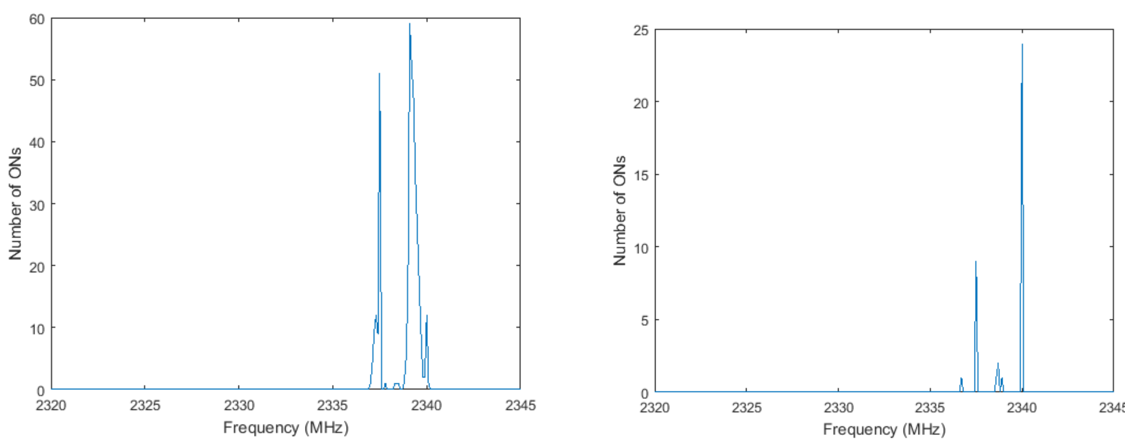


(a) P1a (b) P1b

**Fig. 11.** Number of ON bins in Band 3 in the NIST Machine Shop ($\mu = -80\ dBm$)

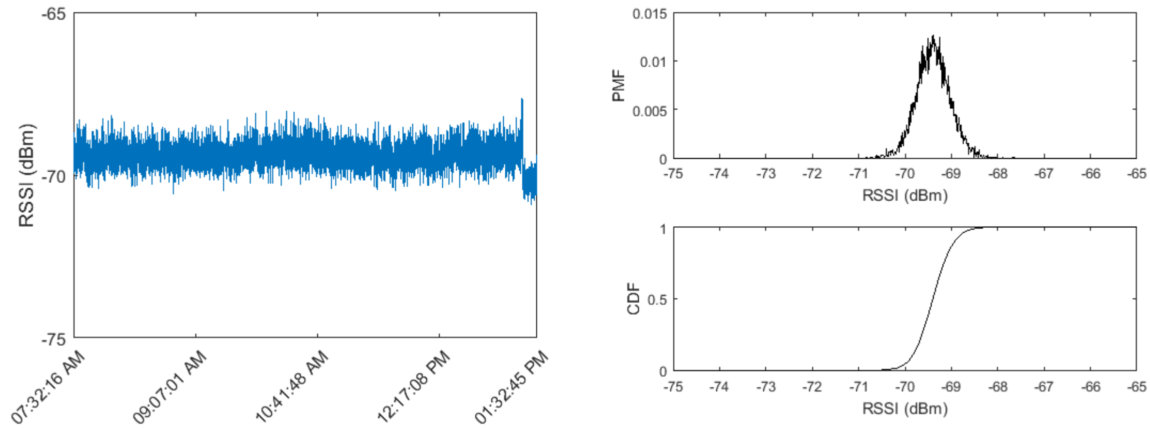


(a) P1a

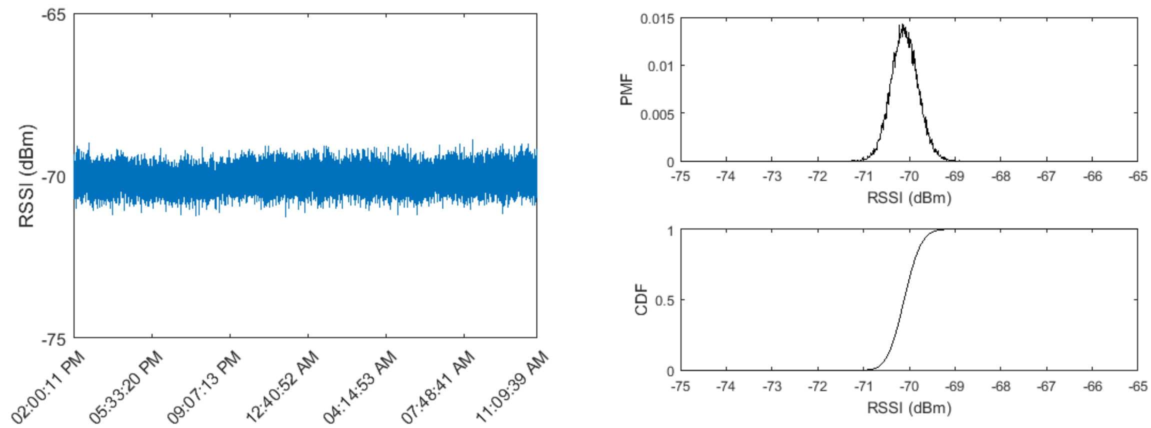


(b) P1b

**Fig. 12.** Time variations (LEFT Col.) and statistics (RIGHT Col.) of RSSI in Band 3 in NIST machine shop

## 2.4. Band 4: 2.4 GHz ISM Band

The 2.4 GHz ISM band has a worldwide bandwidth of 100 MHz from 2.4 GHz to 2.5 GHz. Due to its openness and radio propagation features for wireless transmissions, this band is widely used for wireless networks including IEEE 802.11, IEEE 802.15.4 and their variants. However, it is not clear which type of WLAN is deployed in each facility and what bandwidth it uses. As shown in Table 3, IEEE 802.11 radios may use different bandwidths depending on which physical layer (PHY) technologies they employ. Even with the same WLAN technology, the choice of network configuration, e.g., static channel assignment vs. frequency hopping, can result in different channel loads over the non-overlapping channels. Therefore, our analysis starts from studying the general spectrum usage in this spectrum band.

**Table 3.** Specifications of non-overlapping channels in the 2.4 GHz WLAN in North America (unit: MHz)

| PHY protocol | Channel No. | Center frequency | Frequency range | Bandwidth | |
|---|---|---|---|---|---|
| | | | | Total | Signal subcarrier |
| IEEE 802.11b DSSS PHY | 1 | 2412 | [2401, 2423] | 22 | 22 |
| | 6 | 2437 | [2426, 2448] | | |
| | 11 | 2462 | [2451, 2473] | | |
| IEEE 802.11g/n OFDM PHY | 1 | 2412 | [2402, 2422] | 20 | 16.25 |
| | 6 | 2437 | [2427, 2447] | | |
| | 11 | 2462 | [2452, 2472] | | |

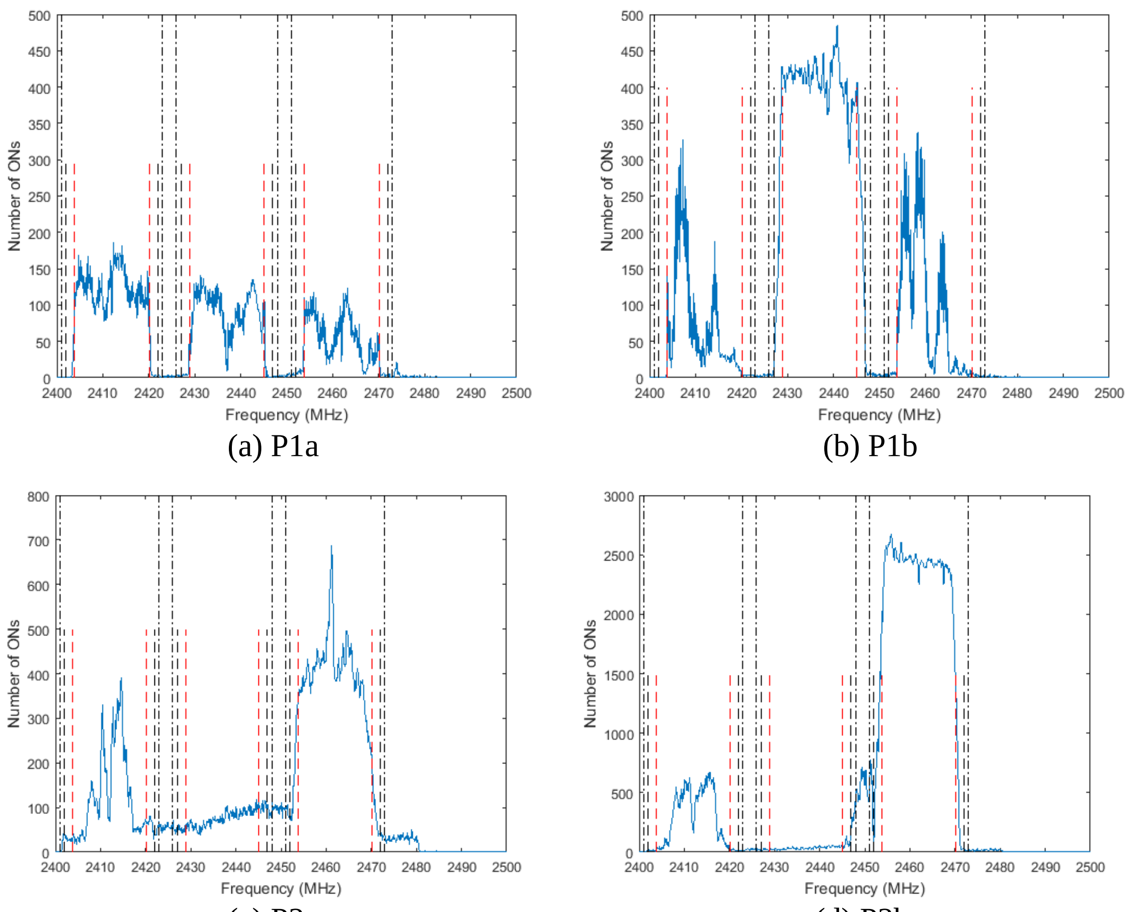


(a) P1a

(b) P1b

(c) P2a

(d) P2b

**Fig. 13.** Number of ON bins in Band 4 at individual listening spots ($\mu = -80\ dBm$)

Figure 13 illustrates the distribution of active signals detected in the 2.4 GHz ISM band at the four listening spots. Walls of the non-overlapping WLAN channels 1, 6, and 11 are plotted to indicate their boundaries and help to identify the type of active WLAN users. There are three sets of boundary lines drawn for each WLAN channel, i.e., the dash-dot lines in black that depict the lower and upper boundaries of the IEEE 802.11b DSSS PHY channels that are 22

MHz wide, the black dashed lines that depict the boundaries of the IEEE 802.11g/n OFDM PHY channels that are 20 MHz wide, and the red dashed lines that depict the boundaries of the real OFDM signal subcarriers that are 16.25 MHz wide.

Figure 13(a) and Figure 13(b) indicate that IEEE 802.11g/n OFDM radios were used at the NIST site because most active bins are detected between the red dashed lines regulating the OFDM PHY channels. As shown in Fig. [13(c), 13(d)], the majority of active signals in the automotive plant fall in the DSSS PHY Channels 1 and 11, even though Fig. [13(c)] shows some activity in Channel 6 as well. However, there are still some notable unrecognized spectrum usage in the ISM band, such as activities beyond 2470 MHz in Fig. [13(c)] and spectrum usage around 2450 MHz in both Fig. [13(c)] and Fig. [13(d)]. Figure 14 compares the time variation of RSSI in the latter frequency range with that in the DSSS PHY Channel 11 at location P2b. Obviously, these activities depict presence of RF signals outside the commonly used WLAN Channels 1, 6, and 11. They are due to non-WLAN radios, such as IEEE 802.15.4 radios, or from WLAN radios that used channels other than those commonly used.

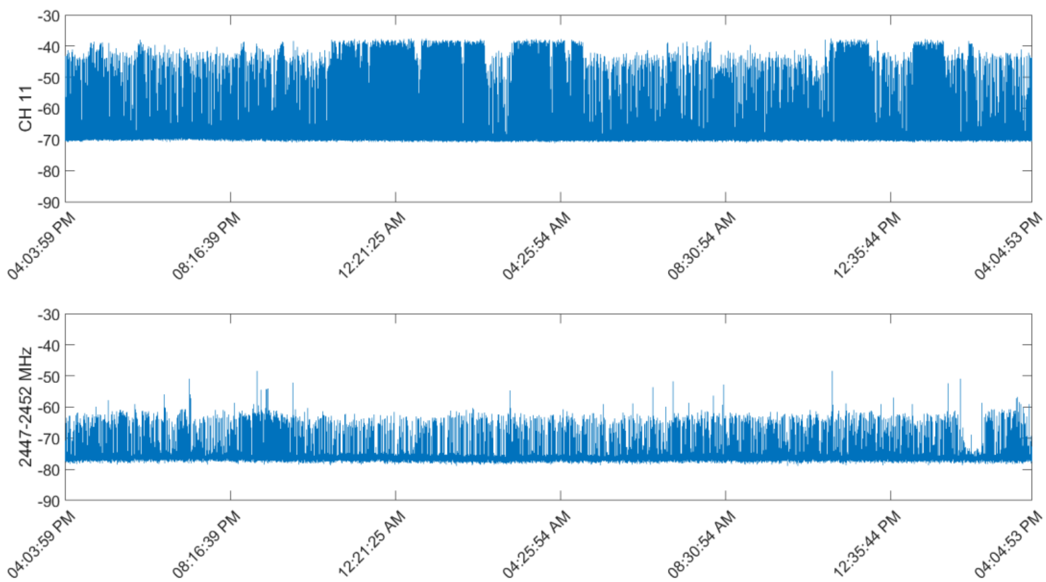


**Fig. 14.** Time variations of RSSI (dBm) in the IEEE 802.11b DSSS Channel 11 and the unrecognized activity in the 2447 MHz to 2452 MHz range at Loc. P2b

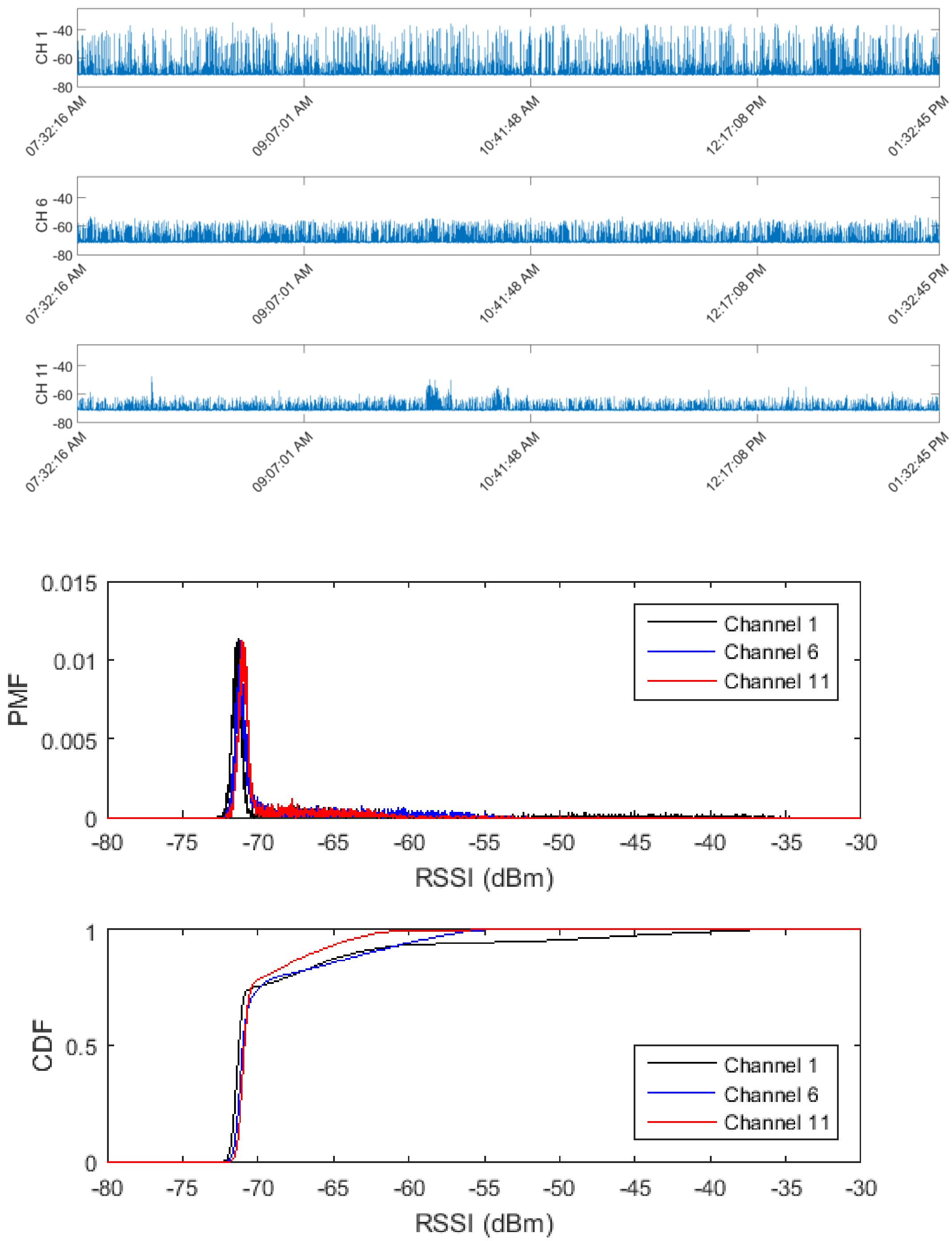


(a) P1a (IEEE 802.11g/n OFDM 20 MHz channels)

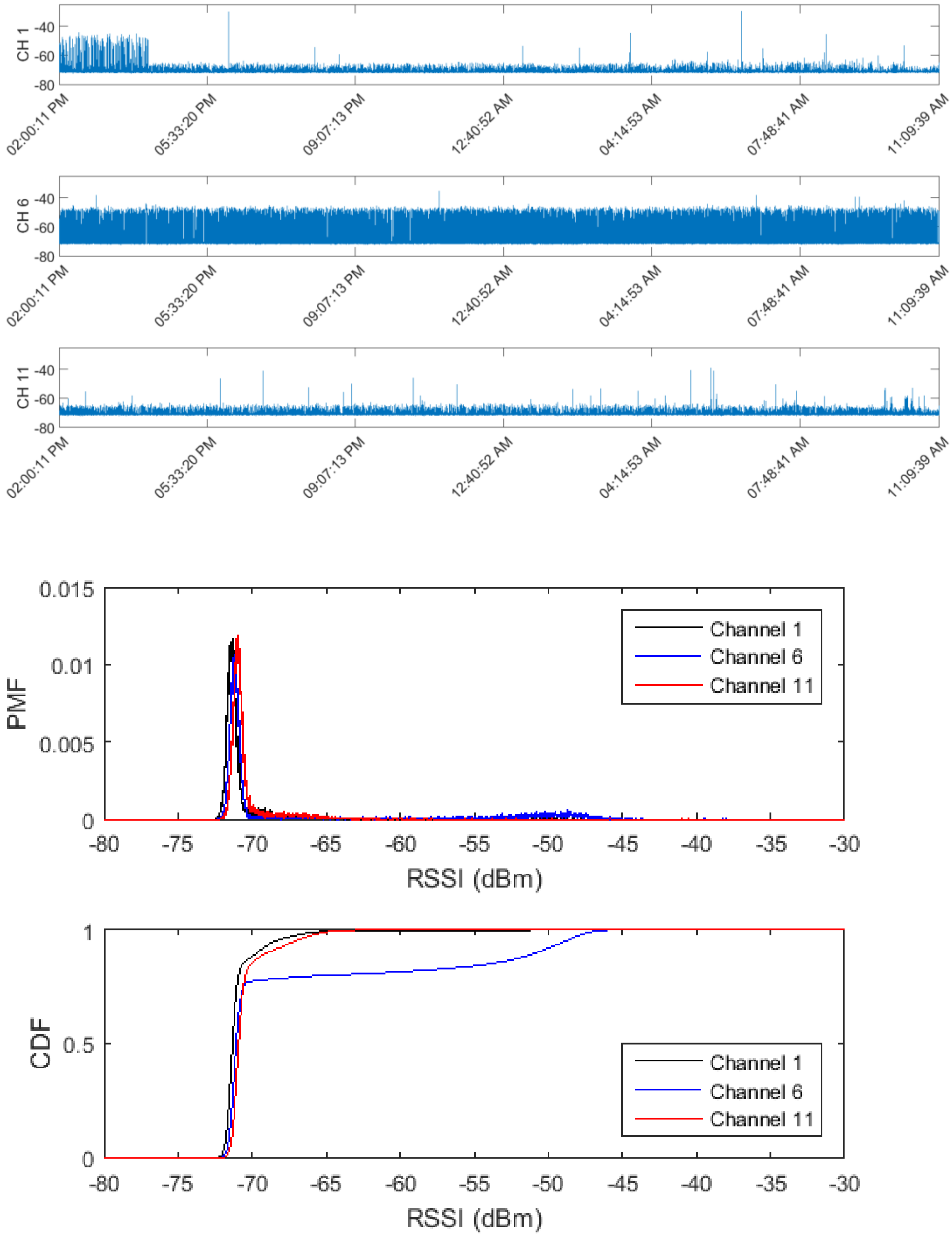


(b) P1b (IEEE 802.11g/n OFDM 20 MHz channels)

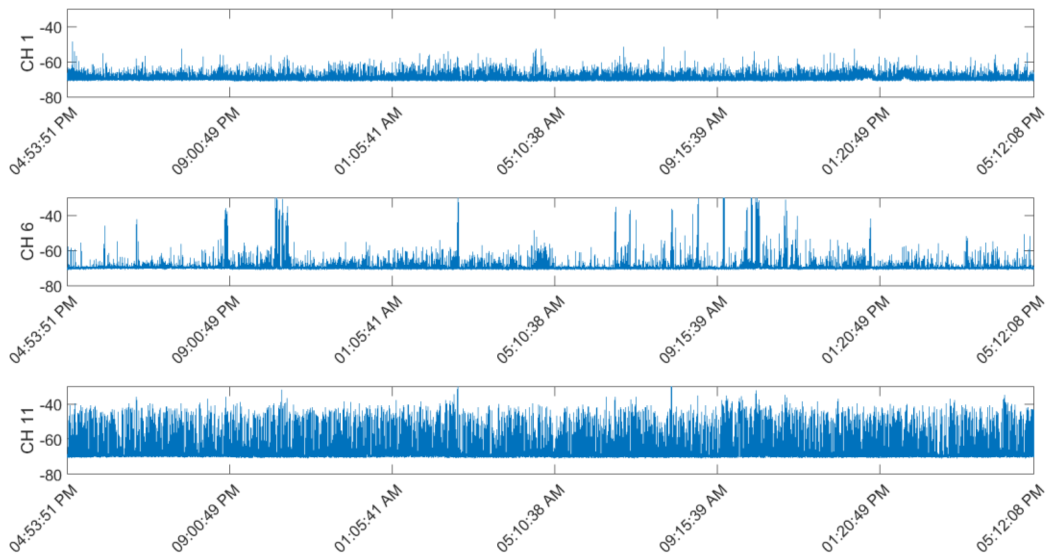


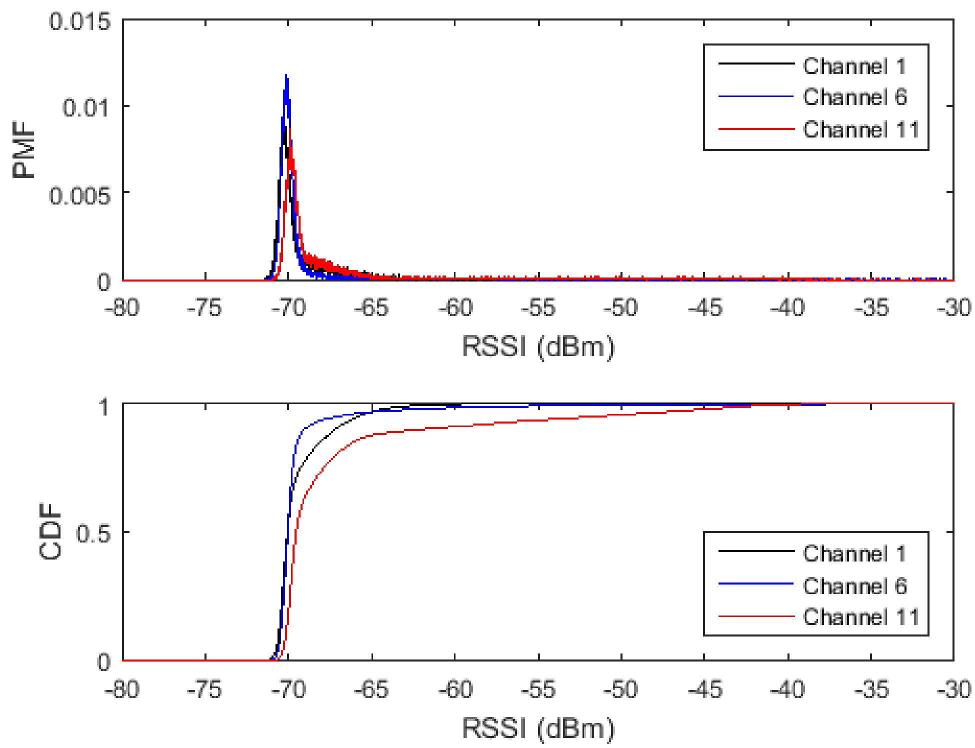


(c) P2a (IEEE 802.11b DSSS 22 MHz channels)

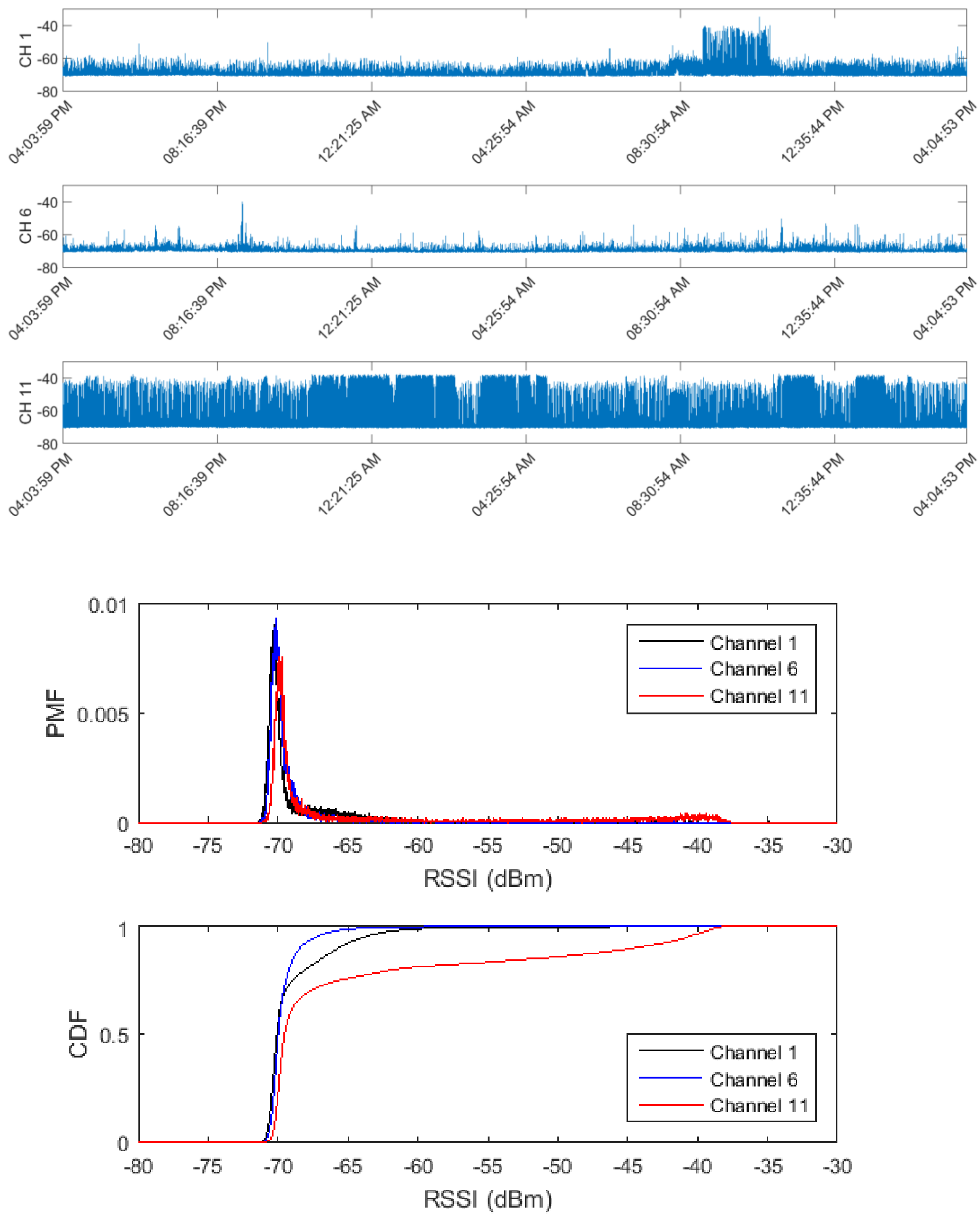


(d) P2b (IEEE 802.11b DSSS 22 MHz channels)

**Fig. 15.** Time variations (Upper) and statistics (Lower) of RSSI in the 2.4 GHz ISM band at various listening spots

Wireless activities have been observed in all three non-overlapping WLAN channels as shown in Fig. [15]. Spectrum usage varies with channel and time of the day.

Two Wi-Fi access points (APs) had been installed in the NIST Machine Shop days before these measurements were made. Therefore, since there were two APs and two listening locations, there would be four RF propagation channels. (We ignore the uplink transmissions and the effects of any Wi-Fi clients.) Figure 15(a) suggests there was light usage of Channel 1 at Loc. P1a between 7:30 AM and 1:30 PM. Figure 15(b) suggests that that light usage came to an end around 4 PM, which is the time many working at the NIST Machine Shop go home at the end of the work day. Note that the Channel 1 signal was as strong at Loc. P1b as it was at Loc. P1a. Figure 15(b) also suggests there was moderate around the clock usage of Channel 6 at Loc. P1b. However, this signal was stronger at Loc. P1b than it was at Loc. P1a. These two figures suggest that Channel 11 was not in use in the NIST Machine Shop, which makes sense because two APs can use at most two channels. We do know that the Wi-Fi APs at NIST are controlled in a centralized manner that uses dynamic channel assignment. They also change their transmit power levels depending on data traffic patterns.

Unfortunately, we do not know how many Wi-Fi APs were present and operational at the automotive transmission assembly plant. Figure 15(c) suggests that at Loc. P2a there were no activity over Channel 1, sporadic activity over Channel 6, and moderate activity over Channel 11. Figure 15(d) suggests that at Loc. P2b there were no activity over Channels 1 and 6, except for a burst of activity over Channel 1 between roughly 9 AM and 10:40 AM, and moderate to at times fairly heavy usage of Channel 11. We do not know whether the APs at the automotive plant are set to operate on fixed channels or are allowed to switch channels.

The received signal strength is affected by channel access intensity. In other words, when a channel is busy, WLAN devices raise their transmit powers for better signal reception following power control rules. To gain more insight into these aspects, we set a channel RSSI threshold at -65 dBm and record the ratio of measurement slots that have a higher RSSI than this threshold and the average RSSI of such slots. Results shown in Table 4 agree with the assumption that the busier bands experienced more signals with higher average RSSI values. Although the ISM band appears to be heavily used, there is still a good chance of finding available spectrum resources in this band given the existing network load in both plants.

**Table 4.** Results of counting sweeps with high RSSI (larger than or equal to -65 dBm) in various WLAN channels and listening spots

| Location | | Channel | Total Sweeps | Sweeps of High RSSI | Ratio of Sweeps of High RSSI | Average RSSI of Sweeps of High RSSI (dBm) |
|---|---|---|---|---|---|---|
| NIST machine shop | P1a | 1 | 9147 | 1163 | 12.71% | -54.86 |
| | | 6 | | 1306 | 14.28% | -60.61 |
| | | 11 | | 632 | 6.91% | -62.71 |
| | P1b | 1 | 32141 | 261 | 0.81% | -55.60 |
| | | 6 | | 6468 | 20.12% | -52.00 |
| | | 11 | | 355 | 1.10% | -62.98 |
| Automotive transmission assembly plant | P2a | 1 | 35764 | 1153 | 3.22% | -62.98 |
| | | 6 | | 1194 | 3.34% | -56.32 |
| | | 11 | | 4418 | 12.35% | -53.61 |
| | P2b | 1 | 35207 | 2774 | 7.88% | -61.79 |
| | | 6 | | 443 | 1.26% | -61.83 |

| Location | | Channel | Total Sweeps | Sweeps of High RSSI | Ratio of Sweeps of High RSSI | Average RSSI of Sweeps of High RSSI (dBm) |
|---|---|---|---|---|---|---|
| | | 11 | | 8481 | 24.09% | -49.54 |

Since the 2.4 GHz ISM band is of special interest for unlicensed wireless devices, further discussions are made in Section 3 with a focus on modelling channel availability in this band.

### 2.5. Band 5: 2655 MHz to 2690 MHz

In the automotive plant, weak signals were captured in the 2655 MHz to 2690 MHz frequency band as shown in Fig. [16]. FCC assigns this band to the services such as radio astronomy, fixed wireless communications and mobile communications, except aeronautical mobile services. Figure 17 indicates that the received signals at both spots were very weak and intermittent. Further analysis on signal features cannot be made until additional data becomes available through future measurement campaigns.

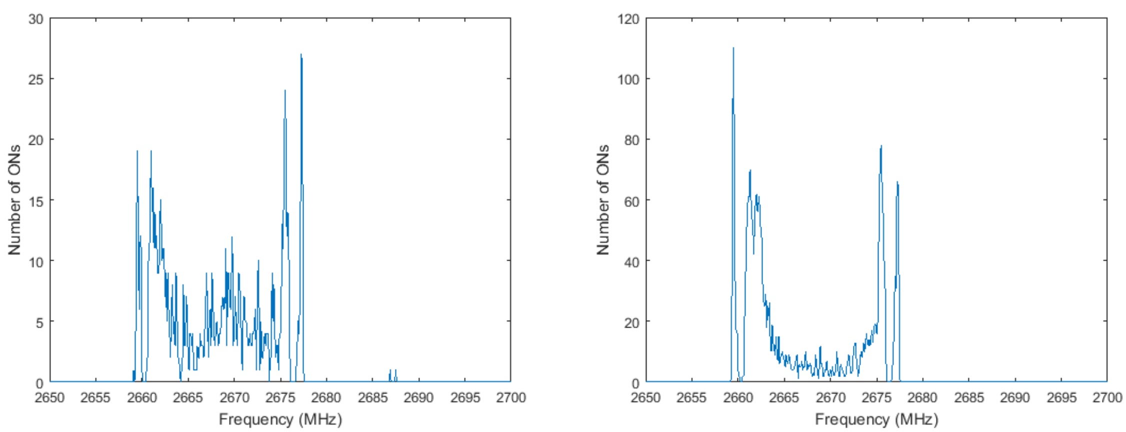


(a) P2a (b) P2b

**Fig. 16.** Number of ON bins in Band 5 in the automotive plant ($\mu = -80\ dBm$)

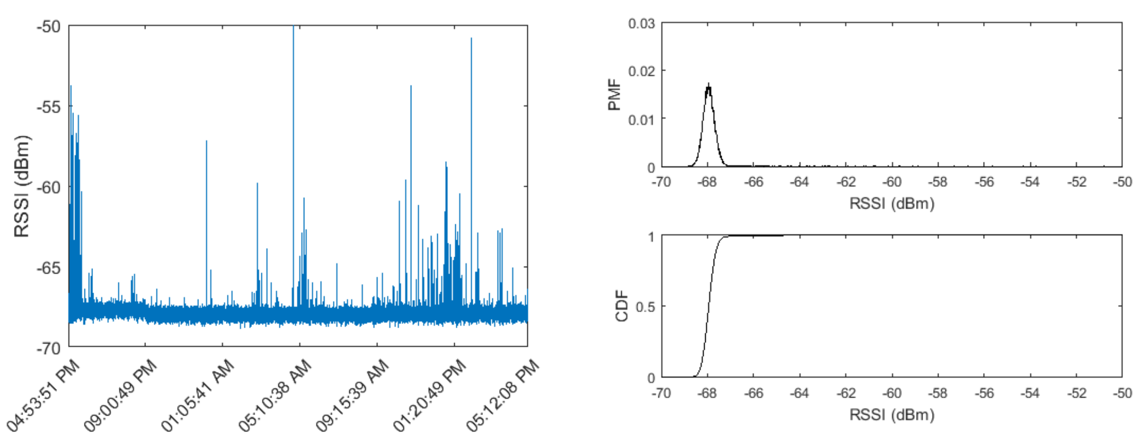


(a) P2a

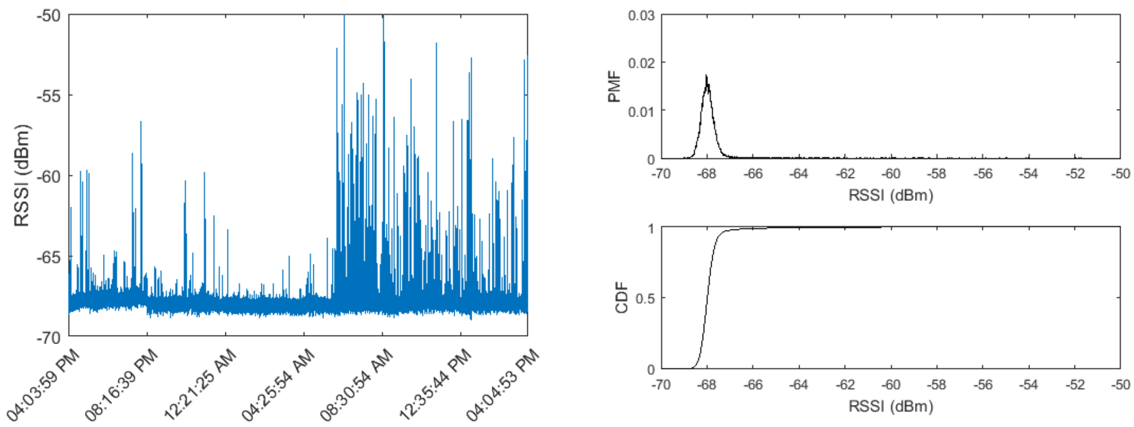


(b) P2b

**Fig. 17.** Time variations (LEFT Col.) and statistics (RIGHT Col.) of RSSI in Band 5 in the automotive plant

As a summary of the wireless usage survey in the frequency range of 2.1 GHz to 2.8 GHz, industrial radio environments are complicated and yet ripe with opportunities for deployment of additional wireless networking technologies.

## 3. Channel Usage Pattern in the 2.4 GHz WLAN Channels

The 2.4 GHz ISM band is unlicensed and has become increasingly popular for new industrial wireless applications that are deployed using Wi-Fi, Bluetooth or IEEE 802.15.4 radios. However, due to spectrum openness, new wireless users in this band have to share the frequency band with existing users, especially in the places where there is a dense concentration of WLAN users. Therefore, coexistence becomes a critical issue to the success of industrial wireless networks. For new players, the first step of deployment is to learn the RF spectrum usage patterns in the target channels. In this section, the RF spectrum usage pattern in the 2.4 GHz WLAN channels is investigated.

The following analysis is conducted in three steps: 1) a binary number is assigned to each channel under study in each measurement time slot to represent channel availability in support of new transmissions; 2) different levels of channel availability and their evolution with time are modeled by a discrete-time Markov chain; 3) channel states are reproduced based on the developed model for further coexistence studies.

### 3.1. ON-OFF Pattern of Channel Availability

Wireless channel availability can be modeled by an alternating ON-OFF random process depending on whether the RF signal power over the frequency band used by the channel is larger than a fixed threshold or not. If a time-slotted wireless system is used in a given channel, from the perspective[4] of any wireless device wishing to transmit in the same channel, the

[4] Note that what is perceived by the wireless device wishing to transmit may not be necessarily the same as the true state of the channel. In other words, with some probability (missed detection probability) the channel will be perceived by the device as being idle, while in reality it is not, and with some other probability (false alarm probability) it will be perceived as being busy, while in reality it is not. This report solely deals with spectrum sensing and the channel state as perceived by the measurement system used at designated listening locations. It does not deal with the true state of the channel.

channel is perceived to be either "busy" (ON) or "idle" (OFF) in each time slot of duration $\Delta t$. It is assumed that the channel stays in the same state[5] (ON or OFF) within each time slot and it either switches with some probability to a different state in the next time slot or stays in the same state. $\Delta t$ is the length of one sweep in our passive measurements, i.e., 2.3 seconds. Wireless devices need to probe the channel before using it to make sure the channel is clear and to avoid causing harmful RF interference to any ongoing transmissions. If the channel is perceived to be idle, the wireless device may start using it. Otherwise, it would defer transmissions for some time. This is called backoff in media access control (MAC) layer protocol terminology. The pattern of channel availability can then be modeled by how likely it is for the channel to be ON or OFF in a given slot, and how long it would remain in the same state. To model the dynamics of channel availability, first we need to have a way of deciding whether the channel is ON or OFF in a given slot.

### 3.1.1. Determining the ON-OFF Threshold

There are two main techniques for deciding whether a wireless channel is busy or idle at a given time. The more sophisticated technique looks for the specific features of the wireless signal, such as the signal constellation or symbol duration, that is expected to be present in the channel. This requires the knowledge of the specific modulation being used by the wireless signal. The simpler technique, which we adopt in this report, is to measure the RF energy received at the listening spot. This is called energy detection.

In each time slot, the channel status is determined by the power/energy level of the received RF signal(s) computed from passively measured RSSIs. Based on RSSI per frequency bin in each sweep, the per channel RSSI is calculated according to Eq. (2) and compared with the ON-OFF threshold, denoted by $\beta_{ON}$. If the per channel RSSI in a slot is larger than $\beta_{ON}$, the slot is marked as ON and the channel state labeled "1"; otherwise the slot is marked as OFF and the state labeled "0". Therefore, $\beta_{ON}$ plays a key role in distinguishing the presence of a signal from background noise when deciding about the channel state. The proper value of $\beta_{ON}$ is determined by the operating conditions, including channel bandwidth, background noise level and receiver sensitivity. For example, under the same conditions and assuming white noise, $\beta_{ON}$ for a 22 MHz channel is expected to be slightly larger than that for a 20 MHz channel.

In practice, different criteria are used to determine $\beta_{ON}$, including device-based clear channel assessment (CCA) and measurement-based noise exclusion. In the former case, as suggested by Cisco, the CCA threshold is determined based on radio sensitivity, e.g., -65 dBm for IEEE 802.11b/g channels [6]. In the latter case, $\beta_{ON}$ is tuned to filter out the majority of noise-only slots and keep most ON slots with active signals. In this report, the noise exclusion method is used to obtain $\beta_{ON}$ at various listening spots to understand the local channel use patterns.

[5] This is an idealization. In reality, transitions can take place within a time slot, because the WLAN uses a CSMA/CA MAC protocol; it does not operate in a time slotted manner. However, we are primarily interested in transmission opportunities for new wireless devices that last several time slots. Hence, it is not critical if we get the beginning or the end of such opportunities off by fractions of a time slot.

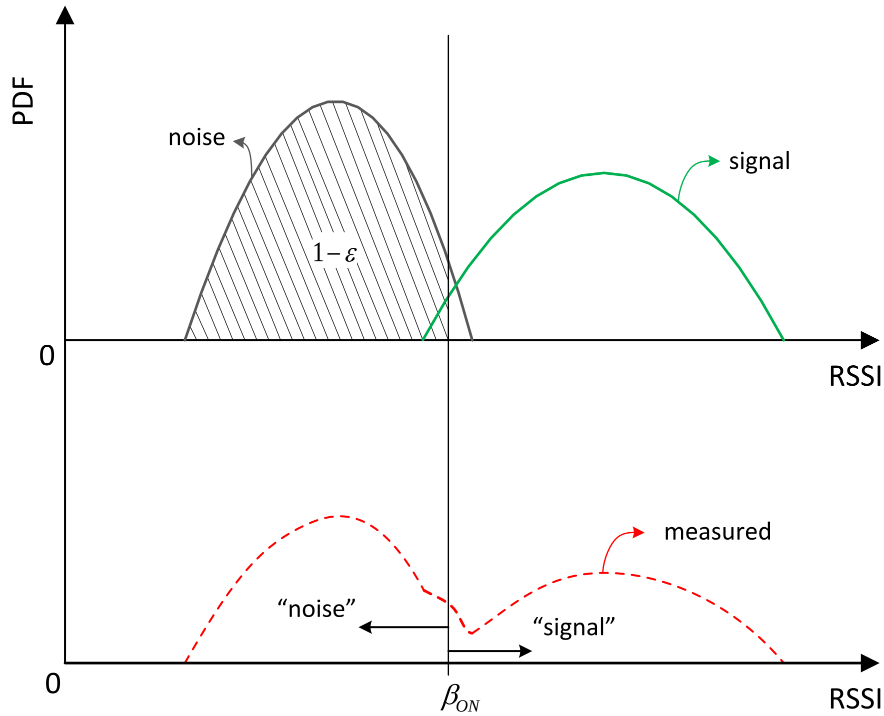


**Fig. 18.** Relationship between $\beta_{ON}$ and $\varepsilon$ in noise exclusion

The signal and noise RSSI probability distributions may partially overlap in a channel, as shown in Fig. [18], and this would pose a challenge to determining $\beta_{ON}$. The first step in the noise exclusion method is to estimate the probability distribution of the per channel RSSI for the background noise. We assume the noise is white, or at least it has a flat power spectral density over and in the vicinity of the RF spectrum of interest (2400 MHz to 2480 MHz). As the probability distribution of the per channel RSSI for the signal is unknown, the measurement data itself cannot directly reveal whether a bin in a given sweep contains signal plus noise or noise only. Therefore, an approximation method is used to obtain the probability distribution of per channel RSSI due to noise only. As discussed in Section 2, there are many "silent" frequency bands in the RF spectrum of interest. In light of the white noise assumption, the probability distribution of the per channel RSSI in these "silent" bands more or less indicative of the noise level at the listening spot in other frequency bands of interest that may have active RF transmissions. This makes it possible to approximate the noise level in other channels with signals present. The 2490 MHz to 2500 MHz frequency band is rarely used at either measurement site while it is next to the populated WLAN channels as indicated in Fig. [13]. Therefore, it is selected as the reference band for the noise approximation in the WLAN channels.

The RSSI of noise in different frequency bins are assumed to be independent and identically distributed (i.i.d.) random variables. The mean $\mu$ and variance $\sigma^2$ of this distribution can be estimated by the mean and variance of the per-bin RSSI measured in the reference band with noise only, which are denoted by $\bar{\mu}$ and $\bar{\sigma}^2$, respectively. The RSSI of a noise-only channel (in the unit of $mW$) is then modeled as the sum of $n$ i.i.d. random variables where $n$ is the number of bins in the channel. By the central limit theorem, the distribution of the sum of $n$ i.i.d. random variables converges to the normal distribution $N(n\mu, n\sigma^2)$ for sufficiently large $n$. Our experiments have shown that the convergence is fast. When $n \geq 50$, the distribution of the RSSI in the noise-only channel can be approximated by the normal distribution $N(n\bar{\mu}, n\bar{\sigma}^2)$. Therefore, such an approximation holds in a WLAN channel with the bandwidth of 20 MHz (in the OFDM physical layer) or 22 MHz (in the DSSS physical layer).

Once the noise RSSI distribution is estimated in a channel, $\beta_{ON}$ can be obtained through the formula $\beta_{ON} = n\bar{\mu} + \sqrt{2n\bar{\sigma}^2}\,\mathrm{erf}^{-1}(2(1-\epsilon)-1)$. $\varepsilon$ is indeed the false alarm probability, that is, the probability that a time slot with noise only is erroneously identified as busy. $\beta_{ON}$ monotonically increases with 1-$\varepsilon$. Selecting a larger $\beta_{ON}$ can cause more interference to existing transmissions, because it becomes more likely for the channel sensing procedure to decide the channel is idle while in reality it is not. On the other hand, selecting a smaller $\beta_{ON}$ can introduce more false alarms by deciding a slot is busy while it is not, which wastes RF spectrum resources. Some researchers propose to dynamically tune $\beta_{ON}$ based on the network conditions for a balance between good usage of the RF spectrum and a low false alarm probability $\varepsilon$. Interested readers may refer to [4] for further details.

Table 5 presents the values of $\beta_{ON}$ for given channel bandwidths and $\varepsilon$'s. In the following discussion, $1-\varepsilon$ is set to 95% so that the majority of idle slots can be checked as OFF.

**Table 5.** Selection of $\beta_{ON}$ (unit: dBm)

| Location | | Bin RSSI (Noise-Only) | | $1-\varepsilon$ | Channel Bandwidth | |
|---|---|---|---|---|---|---|
| | | $\bar{\mu}$ | $\bar{\sigma}$ | | 20 MHz | 22 MHz |
| NIST Machine Shop | P1a | -93.9587 | -94.1614 | 0.95 | -70.4707 | -70.0788 |
| | | | | 0.98 | -70.3644 | -69.9769 |
| | | | | 0.99 | -70.2949 | -69.9103 |
| | P1b | -93.9470 | -94.1545 | 0.95 | -70.4594 | -70.0675 |
| | | | | 0.98 | -70.3532 | -69.9657 |
| | | | | 0.99 | -70.2838 | -69.8992 |
| Automotive Plant | P2a | -93.1997 | -93.2841 | 0.95 | -69.6998 | -69.3084 |
| | | | | 0.98 | -69.5908 | -69.2040 |
| | | | | 0.99 | -69.5197 | -69.1357 |
| | P2b | -93.2527 | -92.1562 | 0.95 | -69.6162 | -69.2305 |
| | | | | 0.98 | -69.4782 | -69.0979 |
| | | | | 0.99 | -69.3885 | -69.0118 |

#### 3.1.2. Statistics of ON/OFF Time Slot Availability

For each WLAN Channel $i \in \{1, 6, 11\}$ and at each listening spot, we used Eq. (2) to compute three sequences per channel RSSI samples $(R_1^i, R_2^i, \dots, R_M^i)$, over M time slots. Using the bandwidth- and location-specific threshold $\beta_{ON}$, the RSSI sequences are converted into three binary sequences $\left(A_1^i,\ A_2^i, \dots, A_M^i\right)$ of length M indicating channel state in the M time slots.
Table 6 illustrates the utilization of WLAN channels at the two industrial plants measurements were made at. It indicates there are still plenty of radio resources available, which is good news for deployment of new wireless technologies in the WLAN band. However, this is not the entire story. The lengths of OFF and ON bursts matter greatly. The longer an OFF burst is, the more the opportunity for a new wireless device to transmit in the same band in the same

session. In addition, the longer an ON burst is, the longer the new device has to defer its transmissions. Therefore, the first order probability distribution of OFF and ON states is not adequate and one needs to study the dynamics of state change as well. In the next subsection a statistical model for channel state transitions is proposed.

**Table 6.** Channel utility

| Location | | Bandwidth | $\beta_{ON}$ (1-$\varepsilon$ =0.95) | Utility | | |
|---|---|---|---|---|---|---|
| | | | | Channel 1 | Channel 6 | Channel 11 |
| NIST Machine Shop | P1a | 20 MHz | -70.47 dBm | 25.34% | 30.40% | 25.96% |
| | P1b | 20 MHz | -70.46 dBm | 13.98% | 23.87% | 20.29% |
| Automotive Plant | P2a | 22 MHz | -69.31 dBm | 25.49% | 12.44% | 42.00% |
| | P2b | 22 MHz | -69.23 dBm | 27.39% | 20.42% | 41.65% |

## 3.2. Markov Channel Model

The channel availability in the 2.4 GHz band has been characterized by the binary random variables for individual WLAN channels, i.e., WLAN Channels 1, 6 & 11, in Section 3.1. In each time slot $m = 1, 2, \dots, M$, a vector of three binary random variables $(A_m^1, A_m^6, A_m^{11})$ is used to represent the availability in the three WLAN channels, where for each $i \in \{1, 6, 11\}$, $A_m^i = 0$ and $A_m^i = 1$ indicate that WLAN Channel $i$ is OFF and ON, respectively. From a new wireless user's point of view, the pattern of state changes is of interest so that the user can opportunistically use the free bandwidth to send packets [5]. In order to characterize the time variations of bandwidth in both capacity and frequency, we introduce a discrete-time Markov chain model. Figure 19 illustrates a general Markov chain with $N$ states, where $p_{ij}$denotes the transition probability from state $i$ to state $j$, for $i = 1, 2, \dots, N$ and $j = 1, 2, \dots, N$.

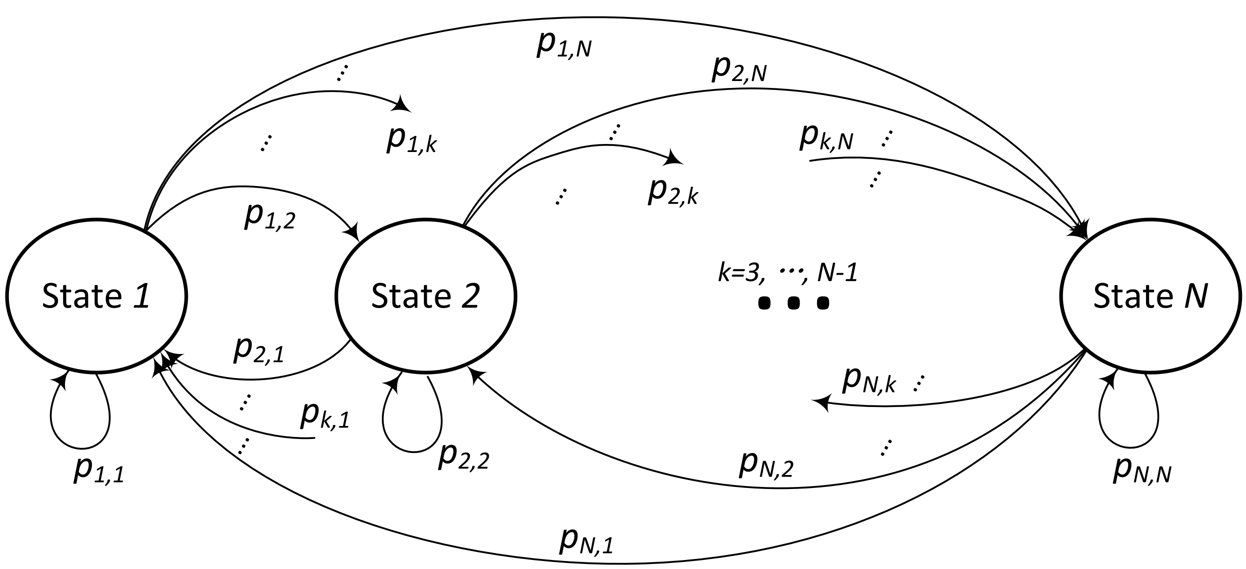


**Fig. 19.** An $N$-state Markov chain model

In our case with three non-overlapping WLAN channels, there are eight possible values for the binary channel state vector $(A_m^1, A_m^6, A_m^{11})$, which results in a Markov chain model with eight states that completely describe the channel availability in time slot $m$. Table 7 defines one possible mapping from the channel ON-OFF vectors to the Markov chain states.

**Table 7.** Mapping of channel ON-OFF status to Markov chain states

| $(A_m^1, A_m^6, A_m^{11})$ | Markov Chain State |
|---|---|
| (0, 0, 0) | 1 |
| (0, 0, 1) | 2 |
| (0, 1, 0) | 3 |
| (0, 1, 1) | 4 |
| (1, 0, 0) | 5 |
| (1, 0, 1) | 6 |
| (1, 1, 0) | 7 |
| (1, 1, 1) | 8 |

Given the measurement data for a specific location, an estimate $\hat{p}_{i,j}$ for the transition probability $p_{i,j}$ can be obtained by

$$\hat{p}_{i,j} = \frac{\#\, Transitions\ from\ State\ i\ to\ State\ j}{\#\, Transitions\ from\ State\ i}, i = 1, \dots, N\ and\ j = 1, \dots, N \tag{3}$$

An estimate $\hat{P}$ of the overall transition probability matrix $P$ is then written as

$$\hat{P} = \begin{bmatrix} \hat{p}_{1,1} & \hat{p}_{1,2} & \cdots & \hat{p}_{1,N} \\ \hat{p}_{2,1} & \hat{p}_{2,2} & & \hat{p}_{2,N} \\ \vdots & & \ddots & \vdots \\ \hat{p}_{N,1} & \hat{p}_{N,2} & \cdots & \hat{p}_{N,N} \end{bmatrix} \tag{4}$$

where $\sum_{j=1}^{N} \hat{p}_{i,j} = 1, \forall i = 1,2, \dots, N$. From this point on, we drop all the ^'s. For example, we use $P$ instead of $\hat{P}$.

The steady state probability distribution $\Pi = [\pi_1, \pi_2, \dots, \pi_N]$ of the Markov chain is the probability that the chain is in a particular state after it has been running for a long time. It can be calculated by solving the following system of linear equations:

$$\begin{cases} \Pi = \Pi \times P \\ \sum_{j=1}^{N} \pi_i = 1, \forall i = 1,2, \dots, N \end{cases} \tag{5}$$

which consists of $N$ independent linear equations.

Based on Eq. (3) - (5), the statistics of the formulated Markov chain model at different measurement locations are listed in Table 8.

**Table 8.** The transition probability matrix $P$ and steady-state probability distribution $\Pi$ at different locations

| | $P$ | | | | | | | | $\Pi^T$ |
|---|---|---|---|---|---|---|---|---|---|
| P1a | 0.3994 | 0.1299 | 0.1631 | 0.0615 | 0.1385 | 0.0413 | 0.0554 | 0.0110 | 0.3790 |
| | 0.3889 | 0.1492 | 0.1460 | 0.0537 | 0.1219 | 0.0545 | 0.0666 | 0.0192 | 0.1362 |

| | | | | | | | | | |
|---|---|---|---|---|---|---|---|---|---|
| | 0.3459 | 0.1368 | 0.1912 | 0.0697 | 0.1421 | 0.0418 | 0.0591 | 0.0133 | 0.1647 |
| | 0.3541 | 0.1426 | 0.1492 | 0.1180 | 0.1262 | 0.0410 | 0.0541 | 0.0148 | 0.0667 |
| | 0.3715 | 0.1360 | 0.1668 | 0.0577 | 0.1597 | 0.0364 | 0.0585 | 0.0134 | 0.1383 |
| | 0.3789 | 0.1418 | 0.1418 | 0.0773 | 0.1392 | 0.0361 | 0.0515 | 0.0335 | 0.0424 |
| | 0.3720 | 0.1308 | 0.1757 | 0.0692 | 0.1364 | 0.0374 | 0.0673 | 0.0112 | 0.0585 |
| | 0.3385 | 0.1538 | 0.1538 | 0.1000 | 0.1000 | 0.0692 | 0.0615 | 0.0231 | 0.0142 |
| P1b | 0.5402 | 0.1262 | 0.1566 | 0.0400 | 0.0821 | 0.0218 | 0.0267 | 0.0064 | 0.5225 |
| | 0.5005 | 0.1630 | 0.1600 | 0.0370 | 0.0870 | 0.0220 | 0.0248 | 0.0058 | 0.1330 |
| | 0.5064 | 0.1273 | 0.1961 | 0.0403 | 0.0776 | 0.0202 | 0.0276 | 0.0046 | 0.1635 |
| | 0.5053 | 0.1339 | 0.1581 | 0.0817 | 0.0681 | 0.0166 | 0.0280 | 0.0083 | 0.0412 |
| | 0.4896 | 0.1417 | 0.1517 | 0.0415 | 0.1191 | 0.0249 | 0.0252 | 0.0063 | 0.0839 |
| | 0.5319 | 0.1333 | 0.1489 | 0.0312 | 0.0738 | 0.0468 | 0.0213 | 0.0128 | 0.0219 |
| | 0.5097 | 0.1317 | 0.1649 | 0.0344 | 0.0767 | 0.0115 | 0.0481 | 0.0229 | 0.0272 |
| | 0.5138 | 0.1009 | 0.2064 | 0.0459 | 0.0321 | 0.0321 | 0.0505 | 0.0183 | 0.0068 |
| P2a | 0.4662 | 0.2464 | 0.0428 | 0.0306 | 0.1244 | 0.0666 | 0.0160 | 0.0070 | 0.3819 |
| | 0.3418 | 0.3559 | 0.0425 | 0.0443 | 0.0970 | 0.0913 | 0.0122 | 0.0150 | 0.2746 |
| | 0.3754 | 0.2355 | 0.0885 | 0.0795 | 0.1004 | 0.0598 | 0.0389 | 0.0221 | 0.0468 |
| | 0.2585 | 0.3115 | 0.0837 | 0.1005 | 0.0871 | 0.0898 | 0.0295 | 0.0395 | 0.0417 |
| | 0.3717 | 0.2027 | 0.0365 | 0.0231 | 0.2068 | 0.1166 | 0.0265 | 0.0160 | 0.1309 |
| | 0.2796 | 0.2800 | 0.0355 | 0.0476 | 0.1718 | 0.1370 | 0.0244 | 0.0241 | 0.0882 |
| | 0.2367 | 0.1819 | 0.1122 | 0.0725 | 0.1915 | 0.0985 | 0.0588 | 0.0479 | 0.0204 |
| | 0.2232 | 0.2486 | 0.0599 | 0.0835 | 0.1488 | 0.1162 | 0.0726 | 0.0472 | 0.0154 |
| P2b | 0.4422 | 0.2270 | 0.0566 | 0.0492 | 0.1231 | 0.0633 | 0.0212 | 0.0175 | 0.3531 |
| | 0.3398 | 0.3138 | 0.0552 | 0.0675 | 0.0979 | 0.0871 | 0.0181 | 0.0207 | 0.2322 |
| | 0.2876 | 0.1786 | 0.1567 | 0.1130 | 0.0911 | 0.0644 | 0.0497 | 0.0589 | 0.0714 |
| | 0.2507 | 0.2200 | 0.1301 | 0.1636 | 0.0814 | 0.0638 | 0.0393 | 0.0511 | 0.0694 |
| | 0.3438 | 0.1836 | 0.0550 | 0.0459 | 0.1995 | 0.1053 | 0.0367 | 0.0302 | 0.1270 |
| | 0.2731 | 0.2252 | 0.0571 | 0.0578 | 0.1714 | 0.1350 | 0.0418 | 0.0384 | 0.0835 |
| | 0.2381 | 0.1186 | 0.0982 | 0.0885 | 0.1540 | 0.1097 | 0.1097 | 0.0832 | 0.0321 |
| | 0.1907 | 0.1671 | 0.1117 | 0.1108 | 0.1299 | 0.1199 | 0.0790 | 0.0908 | 0.0313 |

Table 8 indicates that the 2.4 GHz WLAN band is still underutilized at the two industrial sites we made measurements, because the steady state probabilities of states with no more than one busy channel, i.e., states 1, 2, 3, and 5, add up to anywhere from 0.8 to 0.9. It's also observed that channel availability tends to transition to state 1, where all the three channels are free, as $p_{i,1}$ for any state $i$ usually has the largest value compared with any other transition probability $p_{i,j}$ in the same row of the transition probability matrix $P$. These observations suggest that there are plenty of opportunities for wireless technologies other than WLAN to be deployed in the 2.4 GHz ISM band at these two sites. The new users should scan the ISM band and they will most likely find an available channel to use either immediately or after a short wait and trying again.

The definition of the Markov chain states in Table 9 specifies the individual WLAN channels that are available in each time slot. In practice, as wireless users can explore multiple channels in a frequency hopping manner before each transmission, only the amount of available bandwidth in each slot matters and not which channels. Therefore, we can further reduce the number of channel states by merging several states of the original Markov chain into one state in a new Markov chain defined next.

**Table 9.** Mappings of channel ON-OFF patterns to the states of the new Markov chain

| $(A_m^1, A_m^6, A_m^{11})$ | Channel-Aware State | Capacity-Aware State |
|---|---|---|
| (0, 0, 0) | 1 | 1 |
| (0, 0, 1) | 2 | 2 |
| (0, 1, 0) | 3 | 2 |
| (0, 1, 1) | 4 | 3 |
| (1, 0, 0) | 5 | 2 |
| (1, 0, 1) | 6 | 3 |
| (1, 1, 0) | 7 | 3 |
| (1, 1, 1) | 8 | 4 |

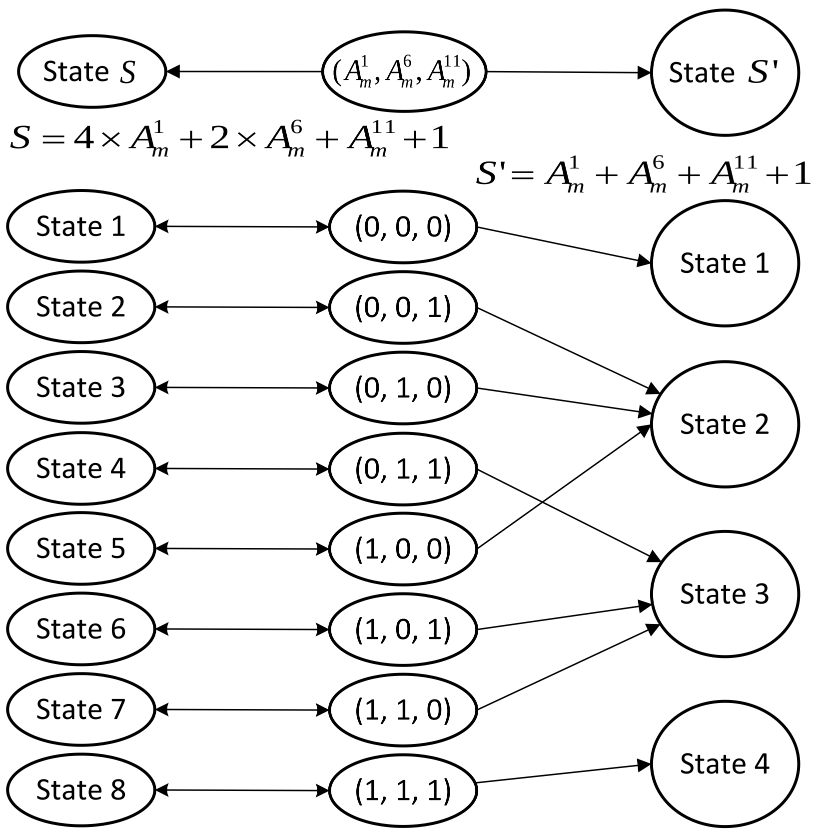


**Fig. 20.** Mappings between channel state vector $(A_m^1, A_m^6, A_m^{11})$, and channel-aware state $S$ or capacity-aware state $S'$, where $4 - S'$ denotes the number of WLAN channels available

Table 9 provides the definitions of two types of channel state used in the original Markov chain and the new one. Each state definition formulates a complete state set by its own to cover all possible channel usage cases in a single time slot. The channel-aware states as proposed in Table 9 make a distinction between channels and specifies precisely which channel is available and which one is not in a given time slot. The new capacity-aware states, on the other hand, focus on only the number of available channels in a given time slot. The mappings from the channel availability vector to both types of states are illustrated in Fig. [20]. Note that only channel-aware states have the inverse mapping to the channel availability vector.

By applying Eq. (3) - (5), we can obtain estimates for the transition probabilities and the steady-state probability distribution of the new Markov chain under the capacity-aware state definition in Table 10.

**Table 10.** The transition probability matrix $P$ and steady-state probability distribution $\Pi$ at different locations under the capacity-aware state definition

| | $P$ | $\Pi^T$ |
|---|---|---|
| P1a | 0.3994 0.4315 0.1582 0.0110<br>0.3673 0.4512 0.1663 0.0152<br>0.3666 0.4279 0.1872 0.0183<br>0.3385 0.4077 0.2308 0.0231 | 0.3790<br>0.4392<br>0.1676<br>0.0142 |
| P1b | 0.5402 0.3649 0.0885 0.0064<br>0.5006 0.4067 0.0873 0.0054<br>0.5131 0.3631 0.1100 0.0138<br>0.5138 0.3394 0.1284 0.0183 | 0.5225<br>0.3805<br>0.0903<br>0.0068 |
| P2a | 0.4662 0.4136 0.1131 0.0070<br>0.3539 0.4738 0.1563 0.0160<br>0.2679 0.4857 0.2148 0.0316<br>0.2232 0.4574 0.2722 0.0472 | 0.3819<br>0.4523<br>0.1504<br>0.0154 |
| P2b | 0.4422 0.4066 0.1337 0.0175<br>0.3323 0.4516 0.1862 0.0298<br>0.2586 0.4310 0.2594 0.0510<br>0.1907 0.4087 0.3097 0.0908 | 0.3531<br>0.4306<br>0.1851<br>0.0313 |

### 3.3. Implementing the Markov Chain Models in Network Design

In this section, we discuss how to implement the Markov chain models developed in the previous section in the study of wireless networks for industrial applications.

#### 3.3.1. Channel Usage Simulation

Under the definition of channel-aware states, given $P$ and $\Pi$, it is possible to simulate the usage of the WLAN channels at each of the four measurement locations studied in this report. The steps are as follows:

1) Generate a random number in the closed interval [0, 1], use it to determine the initial state of the channel in time slot 0, denoted by $s_0$, based on $\Pi$.
2) In time slot $i$, map the state $s_i$ to the channel availability vector, and make those WLAN channels designated by $s_i$ available for use in the current time slot.
3) Generate a random number in the closed interval [0, 1] and use it to determine the next state $s_{i+1}$ of the Markov chain based on the row vector in $P$ corresponding to $s_i$.
4) Jump to time slot $i + 1$, repeat Steps 2) and 3) until the simulation ends.

Figure 21 demonstrates an example of applying the above reproduction steps to simulate the ON-OFF process for the WLAN channels at Location P2a in the automotive plant. The simulated channel availability traces can be utilized in various wireless communication studies, such as channel sensing sequence design, wireless co-existence strategy design, industrial radio environment simulation, and interference management research.

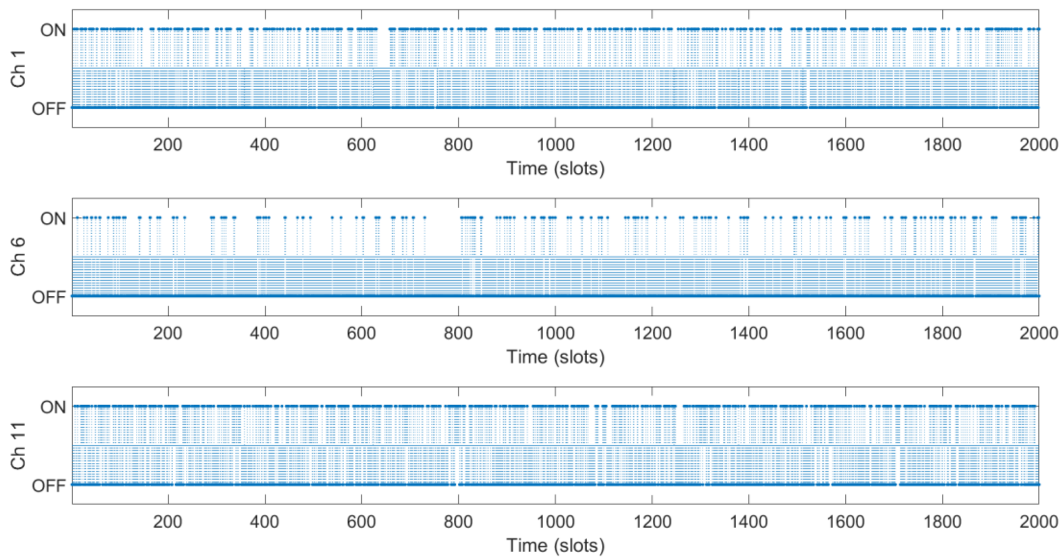


**Fig. 21.** Simulated channel availability traces for WLAN channels at Location P2a with 1-$\varepsilon$=0.95

### 3.3.2. Channel State Estimation

Once a wireless user accesses a free channel in an active communication session, he/she would like to have an idea of how long the channel would be available. On the other hand, if the user finds all the channels busy, he/she would like to know how long to back off and refrain from scanning to look for an available channel. If the channel is highly likely to be in some state, the user can adapt his/her channel access strategy to that state of channel availability. Therefore, channel state estimation is critical to the wireless communications strategy. The Markov chain model introduced in this section can provide insight for better understanding of such issues.

Consider a situation where the "user" is a sensor that needs to transmit its measurements periodically, once every $k$ time slots, and go to sleep in between transmissions to conserve battery usage. The sensor would like to know in which order to sense the three WLAN channels when it wakes up so that it uses the minimal amount of battery power. Let's first look at the channel-aware Markov chain model. If the channel state in slot $m$ is $i$, the probability that the channel state in slot $m+k$, $k \geq 1$ would be $j$, denoted by $p_{i,j}^{(k)}$, is the $(i,j)$ element of the $k$-step forward transition probability matrix

$$P^{(k)} = \underbrace{P \times P \times \ldots \times P}_{k \text{ times}} \tag{6}$$

The sensor can use a number of channel sensing strategies described next:

1. A reasonable WLAN channel sensing strategy is to sense the three channels in the non-increasing order of probability of channel availability in slot $m+k$. Based on the definitions for Markov chain states given in Table 9, we can write

$$
\begin{aligned}
P(A^{1}_{m+k} = 0|S_m = i) &= P(S_{m+k} = 1|S_m = i) + P(S_{m+k} = 2|S_m = i) \\
&\quad + P(S_{m+k} = 3|S_m = i) + P(S_{m+k} = 4|S_m = i) \\
&= p^{(k)}_{i,1} + p^{(k)}_{i,2} + p^{(k)}_{i,3} + p^{(k)}_{i,4} \\
P(A^{6}_{m+k} = 0\big|S_m = i) &= P(S_{m+k} = 1|S_m = i) + P(S_{m+k} = 2|S_m = i) \\
&\quad + P(S_{m+k} = 5|S_m = i) + P(S_{m+k} = 6|S_m = i) \\
&= p^{(k)}_{i,1} + p^{(k)}_{i,2} + p^{(k)}_{i,5} + p^{(k)}_{i,6} \\
P(A^{11}_{m+k} = 0|S_m = i) &= P(S_{m+k} = 1|S_m = i) + P(S_{m+k} = 3|S_m = i) \\
&\quad + P(S_{m+k} = 5|S_m = i) + P(S_{m+k} = 7|S_m = i) \\
&= p^{(k)}_{i,1} + p^{(k)}_{i,3} + p^{(k)}_{i,5} + p^{(k)}_{i,7}
\end{aligned}
$$

The sensor can then sort the three conditional probabilities in a non-increasing order and use that order for channel sensing.

Note that $p^{(k)}_{i,1}$ is a common term in the three expressions given above. Therefore, one can instead compute $p^{(k)}_{i,2} + p^{(k)}_{i,3} + p^{(k)}_{i,4}$, $p^{(k)}_{i,2} + p^{(k)}_{i,5} + p^{(k)}_{i,6}$, and $p^{(k)}_{i,3} + p^{(k)}_{i,5} + p^{(k)}_{i,7}$, and sort these values in non-increasing order.

2. A special case of the previous strategy is when $k$ is sufficiently large. In that case, the knowledge that the Markov chain was in state $i$ in time slot $m$ has little effect on the Markov chain state probability distribution in slot $m + k$, because as $k$ gets larger, the probability distribution for the state in slot $m + k$ converges to the steady-state probability distribution $\Pi$ for the Markov chain. Then elements of $\Pi$ should be used in the three expressions given above instead of elements of $P^{(k)}$.

3. Assume the amount of battery energy consumed is the same no matter which of the three WLAN channels is sensed. Let $D$ denote the number of channels that are sensed before the sensor knows which channel it can use or it finds out that all three channels are busy and none can be used. Another channel sensing strategy is to sense the channels in an order that would minimize $E[D|S_m = i]$. Therefore, the sensor has to compute this conditional expectation for all six possible channel sensing orders and use the order that minimizes $E[D|S_m = i]$.

   Let $(l_1, l_2, l_3)$ be the channel sensing order, i.e. one possible permutation of the set $\{1, 6, 11\}$. Then we can write

$$
\begin{aligned}
E[D|S_m = i] &= 1\times P\left(A^{l_1}_{m+k} = 0\middle|S_m = i\right) + 2\times P\left(A^{l_1}_{m+k} = 1, A^{l_2}_{m+k} = 0\middle|S_m = i\right) \\
&\quad + 3\times\left[1 - P\left(A^{l_1}_{m+k} = 0\middle|S_m = i\right) - P\left(A^{l_1}_{m+k} = 1, A^{l_2}_{m+k} = 0\middle|S_m = i\right)\right] \\
&= 3 - 2\times P\left(A^{l_1}_{m+k} = 0\middle|S_m = i\right) - P\left(A^{l_1}_{m+k} = 1, A^{l_2}_{m+k} = 0\middle|S_m = i\right)
\end{aligned}
$$

   We can now compute this expression for all six possible channel sensing orders

$$E[D|S_m = i]$$
$$= \begin{cases} 3 - 2\times\left(p_{i,1}^{(k)} + p_{i,2}^{(k)} + p_{i,3}^{(k)} + p_{i,4}^{(k)}\right) - \left(p_{i,5}^{(k)} + p_{i,6}^{(k)}\right), & if\ (l_1, l_2, l_3) = (1, 6, 11) \\ 3 - 2\times\left(p_{i,1}^{(k)} + p_{i,1}^{(k)} + p_{i,1}^{(k)} + p_{i,1}^{(k)}\right) - \left(p_{i,5}^{(k)} + p_{i,7}^{(k)}\right), & if\ (l_1, l_2, l_3) = (1, 11, 6) \\ 3 - 2\times\left(p_{i,1}^{(k)} + p_{i,2}^{(k)} + p_{i,5}^{(k)} + p_{i,6}^{(k)}\right) - \left(p_{i,3}^{(k)} + p_{i,4}^{(k)}\right), & if\ (l_1, l_2, l_3) = (6, 1, 11) \\ 3 - 2\times\left(p_{i,1}^{(k)} + p_{i,2}^{(k)} + p_{i,5}^{(k)} + p_{i,6}^{(k)}\right) - \left(p_{i,3}^{(k)} + p_{i,7}^{(k)}\right), & if\ (l_1, l_2, l_3) = (6, 11, 1) \\ 3 - 2\times\left(p_{i,1}^{(k)} + p_{i,3}^{(k)} + p_{i,5}^{(k)} + p_{i,7}^{(k)}\right) - \left(p_{i,2}^{(k)} + p_{i,4}^{(k)}\right), & if\ (l_1, l_2, l_3) = (11, 1, 6) \\ 3 - 2\times\left(p_{i,1}^{(k)} + p_{i,3}^{(k)} + p_{i,5}^{(k)} + p_{i,7}^{(k)}\right) - \left(p_{i,2}^{(k)} + p_{i,6}^{(k)}\right), & if\ (l_1, l_2, l_3) = (11, 6, 1) \end{cases}$$

and select the order that minimizes $E[D|S_m = i]$.

Note that $3 - 2\times p_{i,1}^{(k)}$ is a common term to all the above six expressions. Therefore, one can instead compute $2\times\left(p_{i,2}^{(k)} + p_{i,3}^{(k)} + p_{i,4}^{(k)}\right) - \left(p_{i,5}^{(k)} + p_{i,6}^{(k)}\right)$, $2\times\left(p_{i,1}^{(k)} + p_{i,1}^{(k)} + p_{i,1}^{(k)}\right) - \left(p_{i,5}^{(k)} + p_{i,7}^{(k)}\right)$, $2\times\left(p_{i,2}^{(k)} + p_{i,5}^{(k)} + p_{i,6}^{(k)}\right) - \left(p_{i,3}^{(k)} + p_{i,4}^{(k)}\right)$, $2\times\left(p_{i,2}^{(k)} + p_{i,5}^{(k)} + p_{i,6}^{(k)}\right) - \left(p_{i,3}^{(k)} + p_{i,7}^{(k)}\right)$, $2\times\left(p_{i,3}^{(k)} + p_{i,5}^{(k)} + p_{i,7}^{(k)}\right) - \left(p_{i,2}^{(k)} + p_{i,4}^{(k)}\right)$, and $2\times\left(p_{i,3}^{(k)} + p_{i,5}^{(k)} + p_{i,7}^{(k)}\right) - \left(p_{i,2}^{(k)} + p_{i,6}^{(k)}\right)$ for the six possible orders and select the order with the maximum value.

It is plausible to conjecture that this strategy is equivalent to the first one discussed. That is, if we sense the WLAN channels in the non-increasing order of $P\left(A_{m+k}^{l} = 0 \middle| S_m = i\right)$, we are also minimizing $E[D|S_m = i]$. This conjecture, however, is not true due to the way channel availabilities are related to the Markov chain state definitions.

4. So far, we have discussed fixed channel sensing strategies. That is, we select an order and proceed to sense channels in that order no matter what happens when we sense the first channel. Alternatively, we can decide in which order to sense the remaining two channels after the first one is sensed based on the outcome of the first channel sensed. This leads to the following channel sensing strategy. The first channel to sense should be $l_1 = \arg\max_{n\in\{1,6,11\}} P(A_{m+k}^{n} = 0|S_m = i)$. The second channel to sense should be $l_2 = \arg\max_{n\in\{1,6,11\}-\{l_1\}} P\left(A_{m+k}^{n} = 0 \middle| S_m = i, A_{m+k}^{l_1} = 1\right)$, which is equivalent to $l_2 = \arg\max_{n\in\{1,6,11\}-\{l_1\}} P\left(A_{m+k}^{n} = 0, A_{m+k}^{l_1} = 1 \middle| S_m = i\right)$.

   This leads to $E[D|S_m = i] = 3 - 2\times \max_{n\in\{1,6,11\}} P(A_{m+k}^{n} = 0|S_m = i) - \max_{n\in\{1,6,11\}-\{l_1\}} P\left(A_{m+k}^{n} = 0, A_{m+k}^{l_1} = 1 \middle| S_m = i\right)$.

The premise for the four channel sensing strategies proposed above is the knowledge that $S_m = i$. One way of comparing these four strategies is based on computing

$$E[D] = \sum_{i=1}^{8} P(S_m = i) E[D|S_m = i],$$

which requires the knowledge of $P(S_m = i)$, for $i \in \{1, 2, ..., 8\}$. It is reasonable to use the steady-state probability distribution $\Pi$ of the Markov chain for this purpose.

In the above discussion on channel sensing order, the user does not care about the channel states in the time slots between $m$ and $m + k$. In many cases, however, this does matter. For example, for most wireless transmissions requiring $k$ time slots, it is imperative that "a" channel is continuously available for the entire duration of the transmission, i.e. $k$ time slots. By saying "a" channel, we allow the possibility that the available channel may vary from one time slot to the next over the $k$ time slots needed for the communication session. The capacity-aware Markov chain model can help the user evaluate the likelihood of channel availability in such a case.

As defined in Table 9, states 1, 2, and 3, correspond to the situations where there is at least one channel available in the given time slot. For the user who wishes to have an active session for $k$ consecutive time slots, the channel should stay away from visiting state 4 during the session. In order to compute that probability, we modify the states of the Markov chain. Let $\overline{4}$ indicate any state other than 4, i.e, 1, 2, and 3. Therefore, the transition probability matrix with two states, $\{\overline{4}, 4\}$, is given by

$$P' = \begin{bmatrix} p_{\overline{4},\overline{4}} & p_{\overline{4},4} \\ p_{4,\overline{4}} & p_{4,4} \end{bmatrix} = \begin{bmatrix} \frac{\sum_{i=1}^{3} \pi_i \sum_{j=1}^{3} p_{i,j}}{\sum_{i=1}^{3} \pi_i} & \frac{\sum_{i=1}^{3} \pi_i p_{i,4}}{\sum_{i=1}^{3} \pi_i} \\ \sum_{i=1}^{3} p_{4,i} & p_{4,4} \end{bmatrix} \tag{7}$$

The probability that at least one channel is available in the next $k - 1$ consecutive time slots in addition to current time slot is given by

$$(p_{\overline{4},\overline{4}})^{k-1} = \underbrace{p_{\overline{4},\overline{4}} \times p_{\overline{4},\overline{4}} \times ... \times p_{\overline{4},\overline{4}}}_{k-1 \text{ times}} \tag{8}$$

For instance, for location P1a, $P' = \begin{bmatrix} 0.9859 & 0.0141 \\ 0.9769 & 0.0231 \end{bmatrix}$ and $p_{\overline{4},\overline{4}} = 0.9859$. Hence, it is highly likely to have at least one channel available for a considerable number of time slots. For example, the probability of having at least one channel available for nine more times slots in the future given that one channel is available in the present time slot is $(p_{\overline{4},\overline{4}})^9 = 0.8801$.

## 4. Conclusions

In this report, wireless activities in the 2 GHz spectrum band in industrial environments has been surveyed based on field measurements at two industrial facilities. The temporal variations of frequency band usage and its statistics are investigated. As the 2.4 GHz ISM band is of particular importance to the success of new industrial wireless applications, the channel availability based on existing wireless activities in the 2.4 GHz ISM band is analyzed by using a statistical model.

The findings and modeling methodologies used can be referenced in future studies of industrial wireless networks, especially in wireless coexistence scenarios. Similar approaches can be taken to analyze the passive measurement data in the 5 GHz frequency band, which is available online [1].

Suggestions for future measurement efforts include carrying out 1) longer measurements, e.g., continuous listening for 1 day to 3 days at one single spot so that the variations of wireless usage due to labor shifts can be recorded; 2) measurements with higher time resolution. Each sweep of the 2100 MHz to 2800 MHz frequency band takes about 2.3 s in the measurements this report is based on. It would be desirable to reduce that figure to a fraction of millisecond, perhaps by reducing the width of the frequency band that is being scanned to 20 MHz to 40 MHz, which is the width of a channel in a typical wireless communications standard. A faster sweep rate can do a better job of recognizing the micro-level channel usage patterns at the same level of the carrier sensing operations of current radios. As the CCA in IEEE 802.11 and IEEE 802.15.4 are performed over a few waveform symbols, e.g., 128 $\mu s$ for 8 symbols, if each sweep takes 128 $\mu s$, then our measurement system would be mimicking the CCA operation of the wireless protocol under surveillance.

**References**

[1] NIST (2015) Project Data: Wireless Systems for Industrial Environments, Retrieved Sept. 26, 2017, from http://www.nist.gov/el/isd/cs/wsie_data.cfm
[2] FCC (July 18, 2016) FCC Online Table of Frequency Allocations, Retrieved Sept. 26, 2017, from https://transition.fcc.gov/oet/spectrum/table/fcctable.pdf
[3] CSG Network (August 15, 2011), Satellite S Band Radio Frequency Table, Retrieved July 21, 2016, from http://www.csgnetwork.com/satradiofreq.html
[4] I. Ramachandran and S. Roy (2006) On the impact of clear channel assessment on mac performance, *IEEE Globecom*. https://doi.org/10.1109/GLOCOM.2006.884
[5] D. Striccoli, G. Boggia, and L. A. Grieco (2015) A Markov Model for Characterizing IEEE 802.15.4 MAC Layer in Noisy Environments. *IEEE Transactions on Industrial Electronics* 62(8):5133-5142. https://doi.org/10.1109/TIE.2015.2403792
[6] D. Stiff and M. Rhoades (2011) Spectrum Analyzers are Not All Created Equal, Retrieved Sept. 26, 2017, from https://www.scribd.com/document/61561543/Cisco-CleanAir-Spectrum-Analyzers-Are-Not-All-Created-Equal